PHILIPS

sense and simplicity

State of the Art and Future Trends in Radiation Detection for Computed Tomography

Ami Altman, PhD, PHILIPS Science Fellow
Global Research & Advanced Development
CT BU, PHILIPS Healthcare

PHILIPS

Plan

1. Conventional, state of the art, and future CT detection system

2. A Dual-Layer detector for a Detector- Based Spectral CT, with some applications' examples

3. Photon-Counting Spectral CT detectors, advantages, opportunities, and risks

PHILIPS

A Little About CT

Present CT

1. **Large Coverage Detector**
2. **Wedge Configuration**
3. **Fast Rotation (close to 0.25 sec/Rot.)**
4. **2D Focal-Spot double sampling**
5. **Very Short angular sampling time (~100 μsec)**
6. **High-Rate and Power X-Ray Tubes**
7. **Sub-Millimeter isotropic resolution**
8. **Very good temporal resolution**
9. **A 3D and 4D imaging devise (Space-Time)**

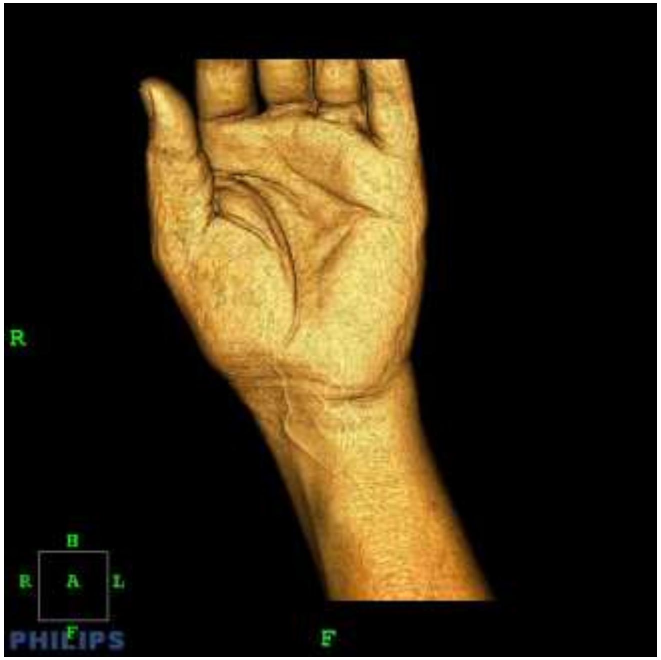

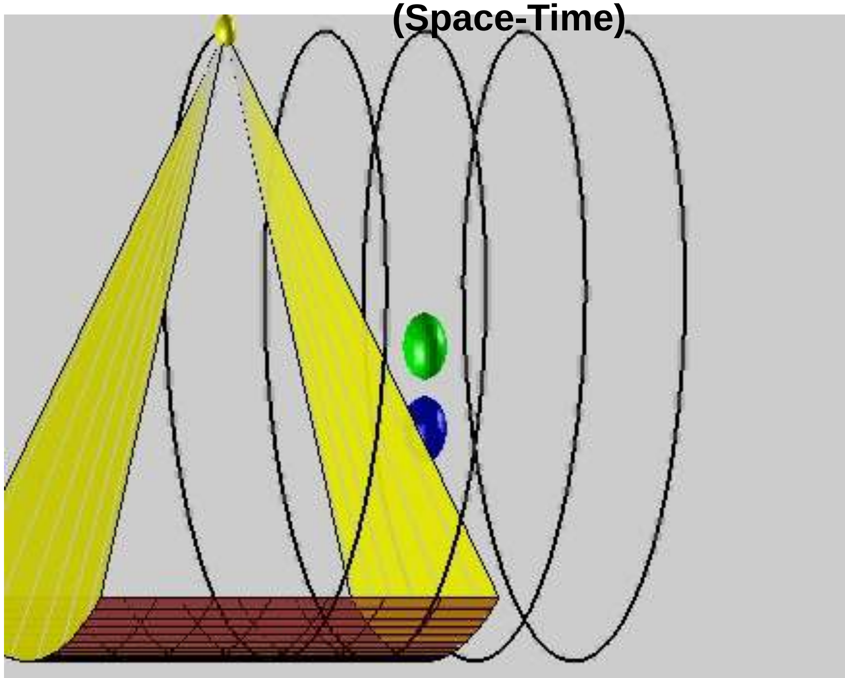

PHILIPS

So How Does It Look Like in Reality?

Detection Array System

Couch

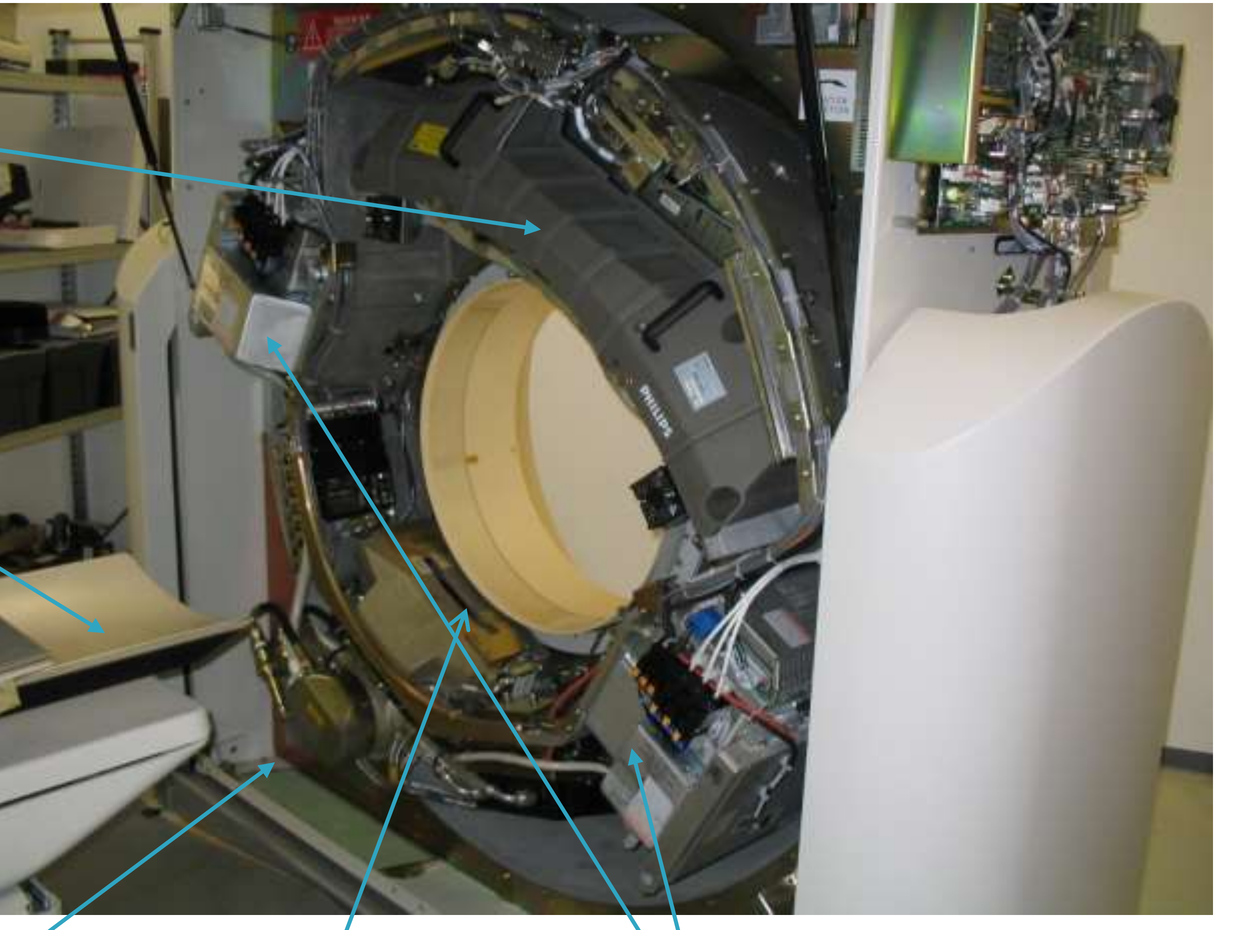

X-Ray Tube

X-Ray Generators

Beam Shaping Collimator

PHILIPS Pixelated CT Detector – Basic Pixel Structure & Requirements

Modern CT Detectors Requirement	
Frame Rate & size	10,000 frames/sec ~120,000 pixels/frame
Detector Readout Mode	Current (energy) Integration
Electronic noise RMS	< 3 pA
High light output scintillator	Ceramic Gd_2O_2S (GOS) (~40,000 photons/MeV)
Low Scintillator Afterglow	<200 ppm at 3 m-sec <20 ppm at 500 m-sec
expandable configuration	4-sides tile-able arrays
Spatial Resolution	~24 lp/cm (~0.210 mm)
Scattering rejection	SPR < 5%; 2D Anti-Scatter-Grid
Maximum Crosstalk (optical & elec)	~5%
Pixelated Si photodiode with excellent response	> 0.35 A/Watt for λ = 514 nm
Dynamic Range	$\geq 2^{20}$
Scintillator Stopping power	> 98% for 120 kVp specctrum

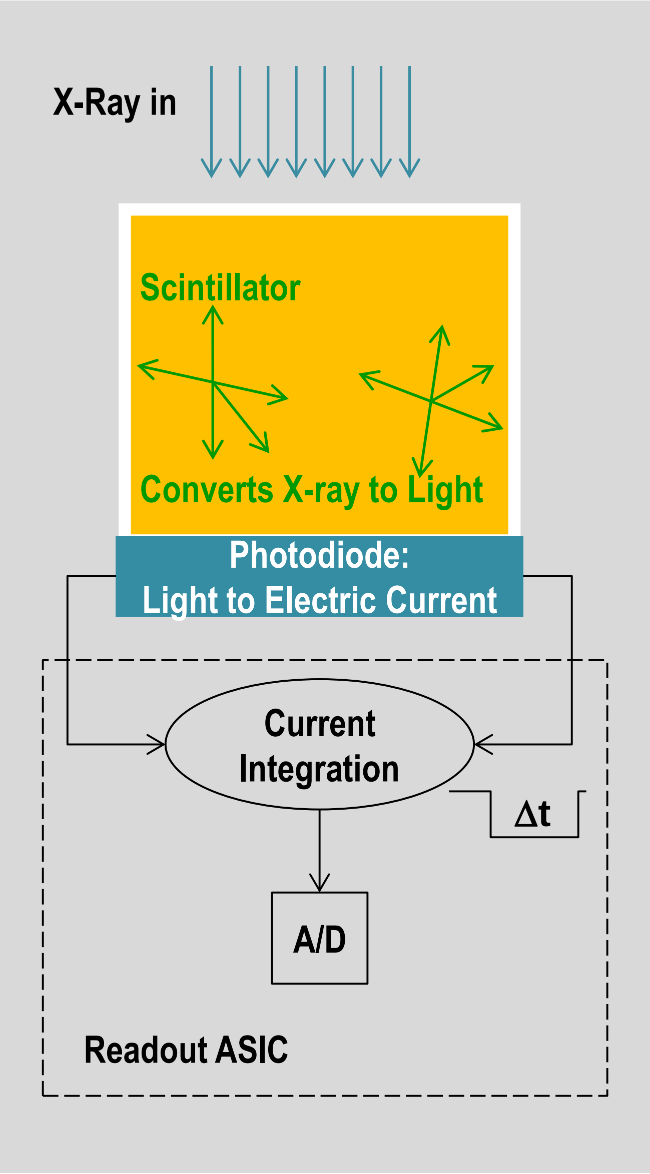

Signal Pixel ∝ Total X-Ray Energy absorbed in the scintillator within a sampling time.

Pixelated Large-Area Photodiode for CT Detector

Back illuminated "64 slices" photodiode "flip-chipped" to a substrate

Front-illuminated photodiode: anodes directly illuminated ; limited expandability

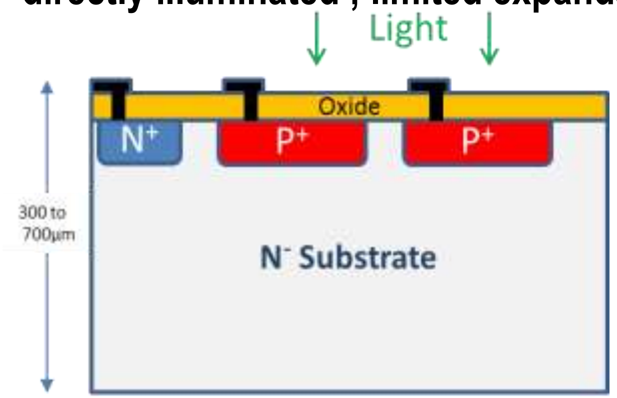

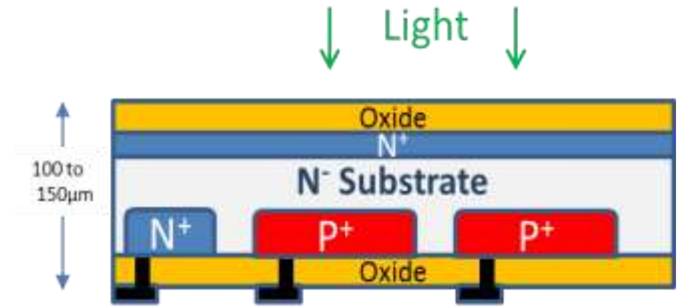

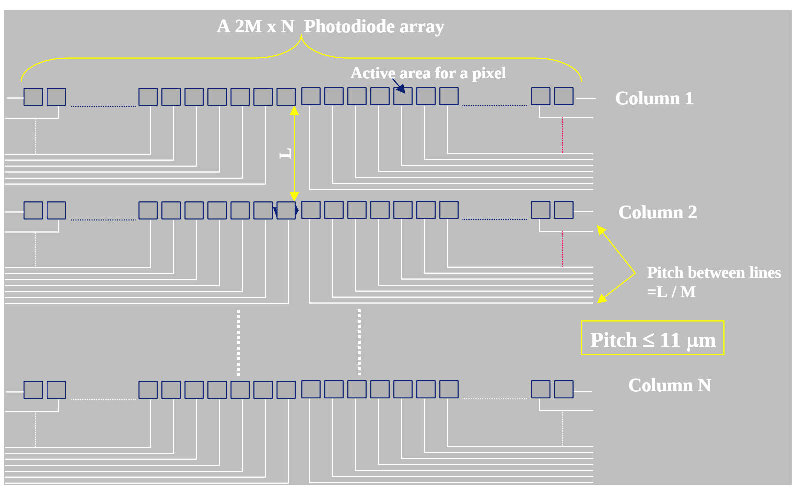

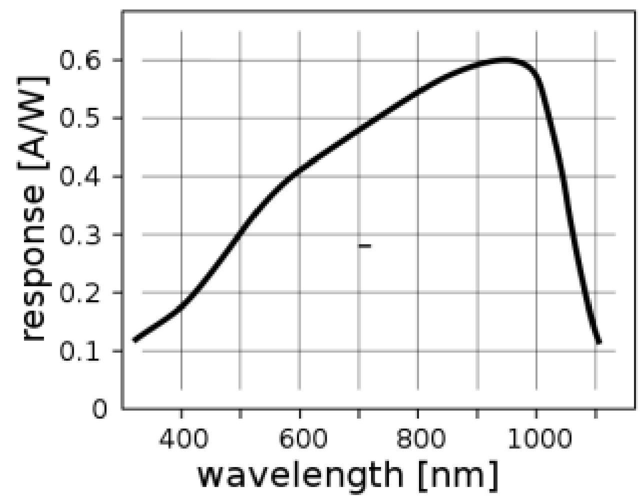

Si Photodiode response

Scintillator Arrays for CT, Material types

CT Scintillators in Use, (Potential Use)				
Scintillator	**Light-yield (# photons/MeV)**	**Form: Ceramic \ Single Cristal**	**Afterglow**	**Comment**
Gd_2O_2S:Pr,Ce (GOS)	~40,000	Ceramic; semi translucent	low	Most vendors; some doping variations
GE Gemstone™ (a Lu based Garnet)	~40,000	Ceramic; translucent	low	
Garnet type of $(Lu,Gd,Y,Tb)_3(Ga,Al)_5O_{12}$	40,000-45,000	Ceramic; translucent	low	Fast rise time
$(Y,Gd)_2O_3$:Eu (GE HiLight™)		Ceramic	high	not adequate for short Integration Periods
ZnSe:Te (low stopping power)	~65,000	Single Cristal; semi-translucent	low	In Philips Dual-Layer CT prototype

$$Light\_Yield\_Limit \cong \frac{10^6}{2.5 \cdot E_g}\ photons/MeV$$

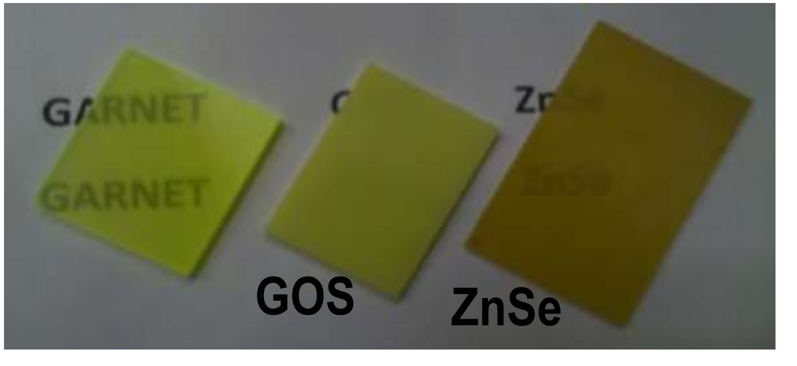

<u>NOTE:</u> Light output is smaller than Light-Yield because of Internal absorption & Reflections

Pixelated Scintillators, and CT DAS Assembly Modes

PHILIPS

Philips Brilliance-64 Module W\O and with anti-scatter grid

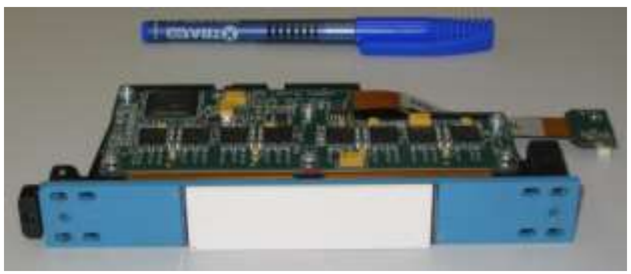

PHILIPS iCT-256, Tiled Config. , 2D anti-scatter grid

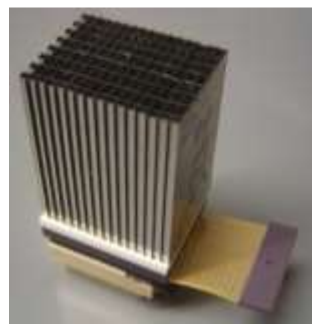

2D-Anti-Scatter grid

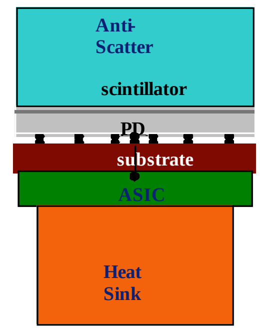

Tile Concept

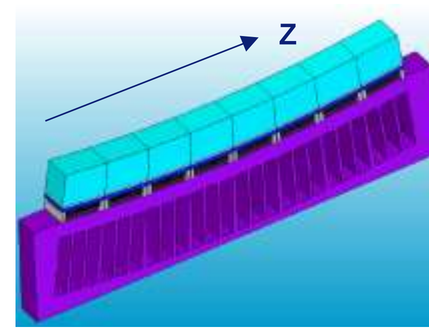

Tiled Module

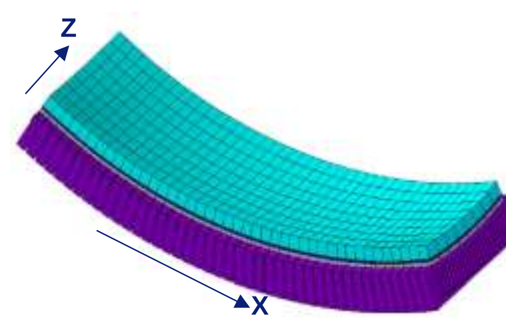

Why Anti Scatter Grids in CT Detectors ?

1. **Detector-Pixel signal at each sampling is assumed to represent a line integral of the form:**
$$P(\phi,\theta)=\ln(I_0)-\ln(I)=\int_{\xi_{in}}^{\xi_{out}}\mu(\xi)d\xi$$
that assumes X-Ray pure-transmission only.

2. **Allowing scattered radiation $\Rightarrow$ Cupping and blackened streaks artifacts between scattering centers:**

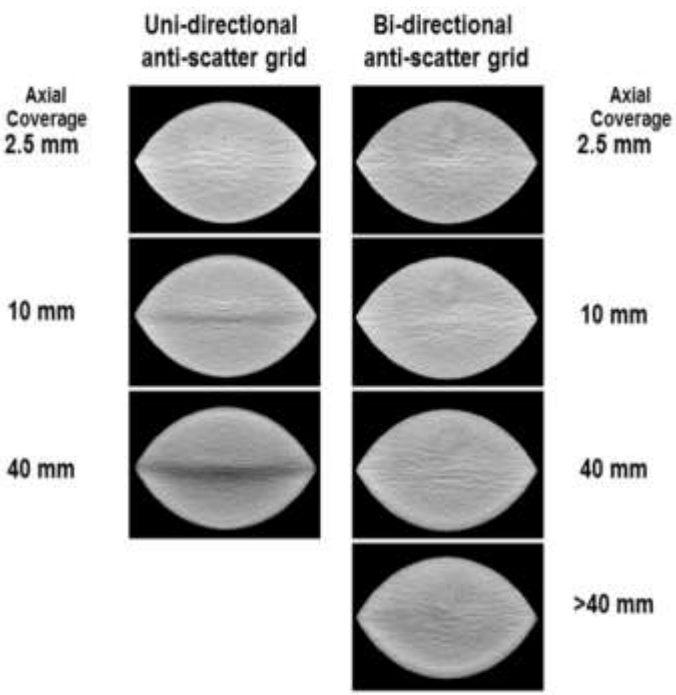

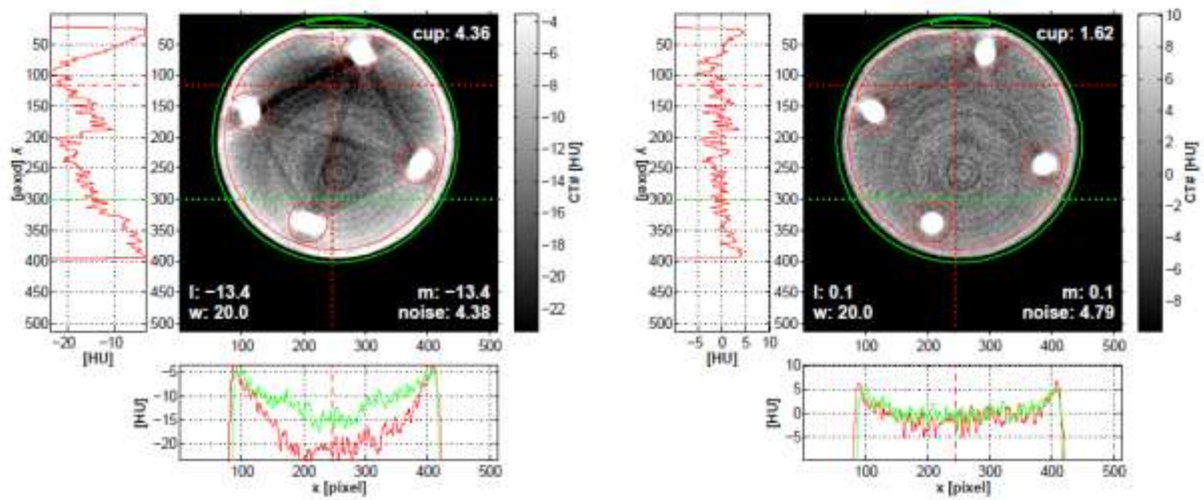

1D VS. 2D Anti-Scatter Grid

SW Scatter-artifacts Correction effect!
Note the significant noise increase.

MTF, DQE and Detection Efficiency, as CT Detectors Metrics

Estimated upper limits of MTF and various CT parameters contribution to it in standard resolution mode (Philips iCT-256), assuming Sinc function response:

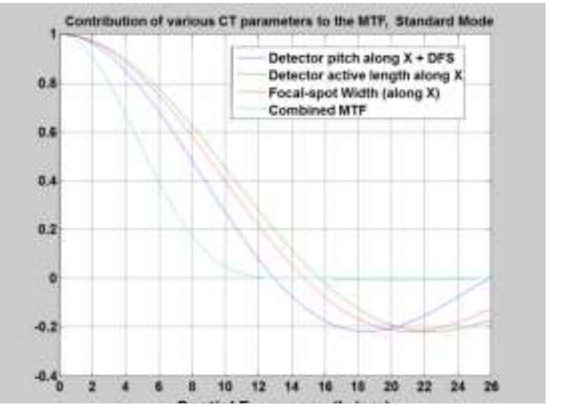

$$DQE = \frac{SNR_{out}^2}{SNR_{in}^2}$$ **, or measured:** $$DQE(f) \cong \frac{S^2\, MTF^2(f)}{NPS(f) \cdot \phi}$$

(S=detector signal; ϕ = # of photons per area unit; NPS= Noise Power Spectrum)

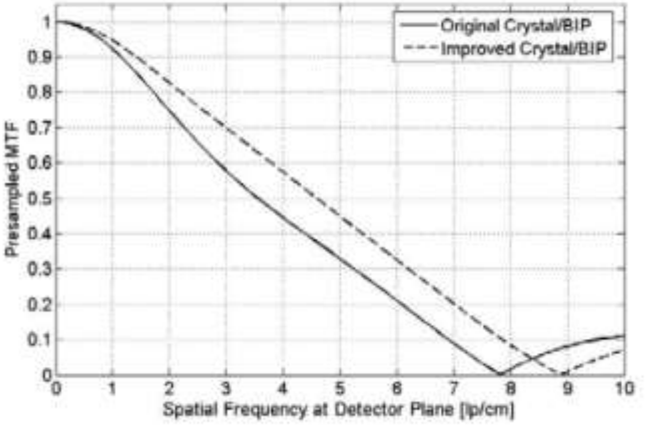

Figure 11: Presampled MTF for two crystal array/BIP configurations.

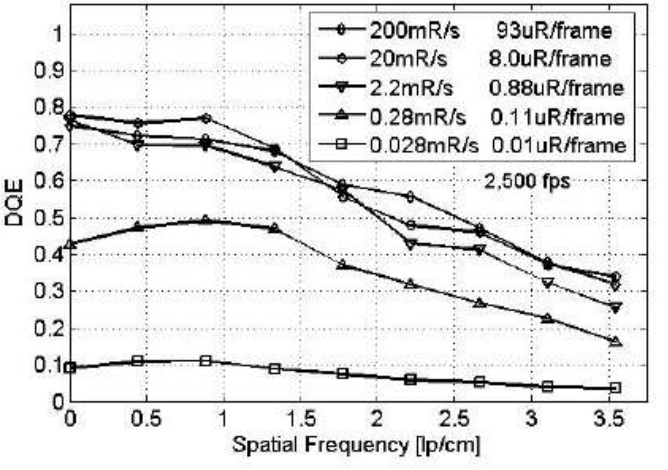

Figure 13: DQE measured at 2500fps for 5 different exposures from 93uR/frame to 0.01uR/frame

A measured single pixel MTF and DQE (PHILIPS tile detector), (including Swank Noise and Crosstalk *(R Luhta et al. SPIE-2006)*

Overall Detection Efficiency (DE) has to include the Geometrical Detection Efficiency (GDE) , determined by the fraction of active area to total pixel area in the pixelated scintillator (~73%).

$$DE = GDE \cdot DQE$$

MTF Improvement – Crosstalk & Afterglow Corrections

Measured Detection-Pixel crosstalk and deviation from pure square wave response due to crosstalk.
(R. Luhta et al, SPIE-2006)

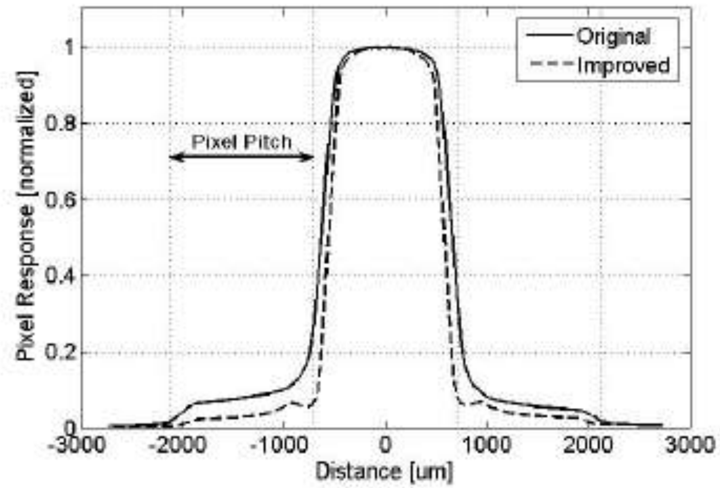

Correcting for Pixel Crosstalk, and Scintillator Afterglow through deconvolution method (Philips Brilliance 16), in an Ultra-High Resolution Mode (slice plane)

(See R. Carmi et al. Nuclear Science Symosiom conference record 2004, 5:2765-2768.)

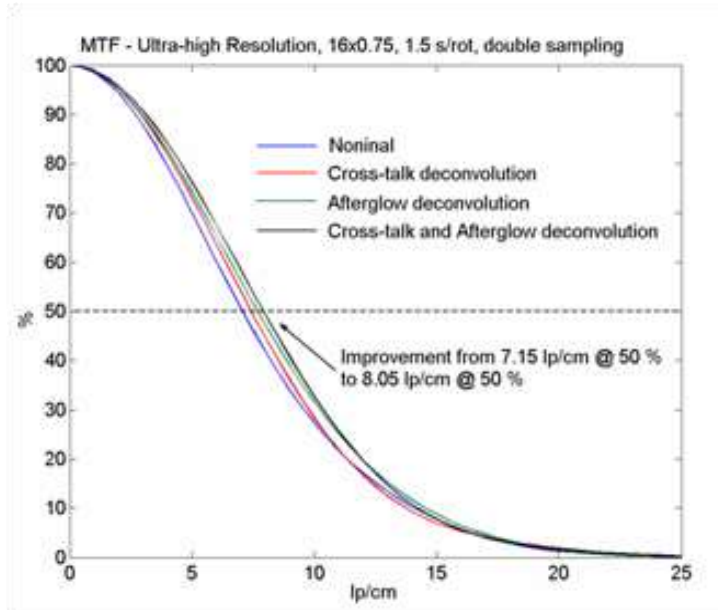

PHILIPS Effect of Electronic Noise in Energy-Integrated CT Detector

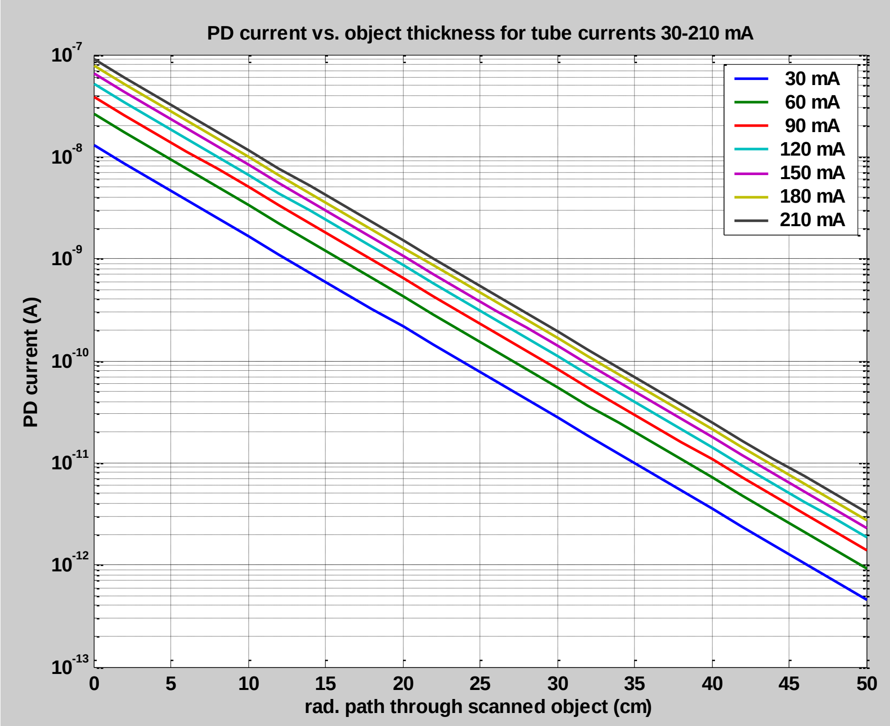

Photodiode's current as a function of absorption path (water), and Tube current

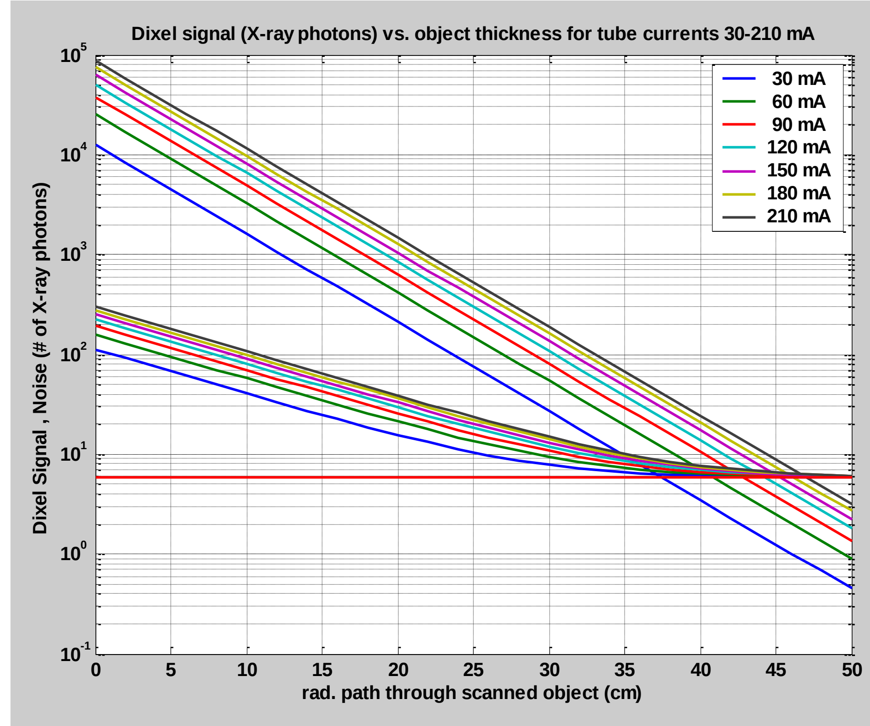

Detector's radiation signal and total noise as a function of absorption path in water, and Tube Current

- **An exaggerated RMS noise of 5 pA has been taken in account, just for demonstration**
- **Today's readout ASICS which are assembled attached to the photodiodes have RMS noise < 3 pA**
- **In most read-out electronics, both Sigma-Delta, or Current-to-Frequency, the RMS noise increases slightly for shorter integration periods**

PHILIPS

Low Dose Artifacts (rings), introduced by Electronic Noise and Non-Linear Effects

1. **50-cm water phantom**
2. **Old version Electronics Philips BR-64 (non-tiled)**
3. **Scanned at 0.4 sec/rot., with 70 mAs**
4. **Measured RMS noise ~5pA**
5. **Artifacts caused mainly by electronics non-linear effects and offset stability during the scan**

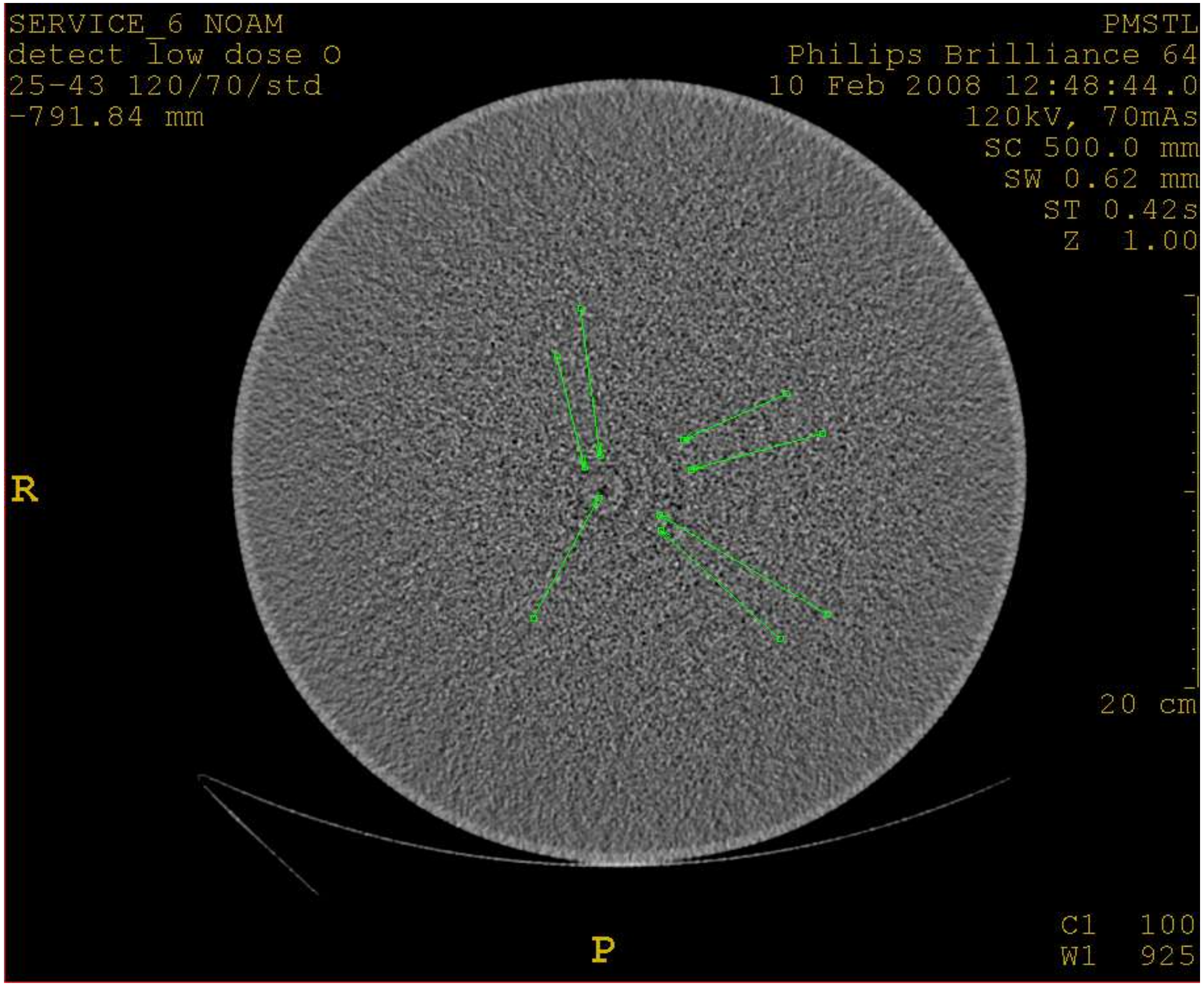

Dual-Energy Spectral CT Based on A Dual-Layer Detector

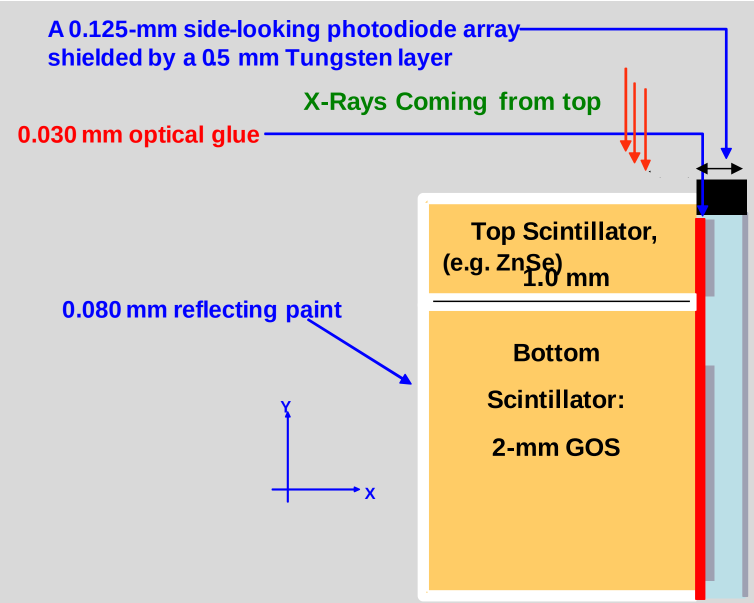

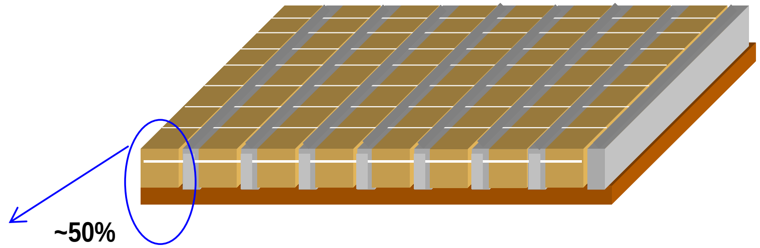

~50%

Low Energy Raw data → E1 image

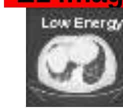

+

~50%

High Energy Raw data → E2 image

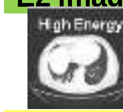

=

Weighted combined Raw data → CT image

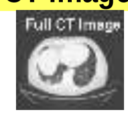

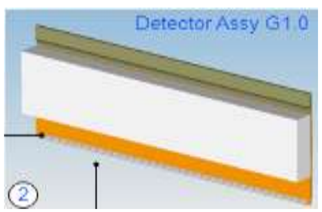

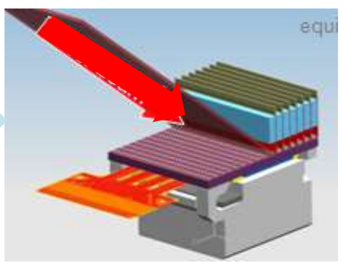

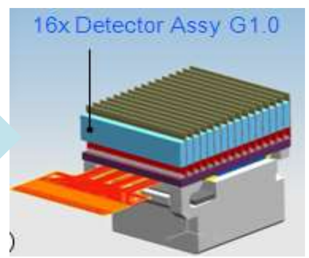

Stacking Dual-Layer 1-D arrays into a single standard detection tile

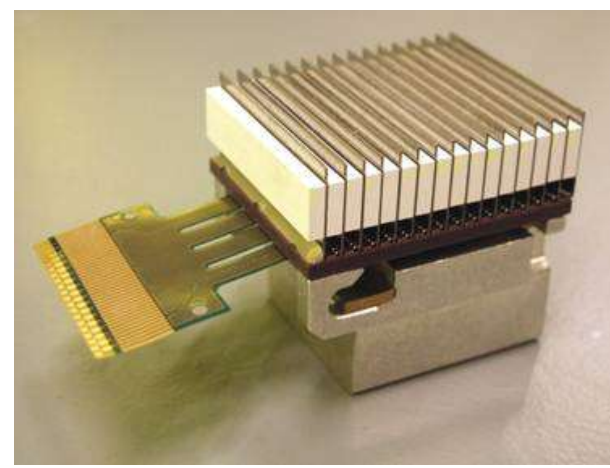

A 16 X 16 pixels Dual-Layer Detector Tile for A Dual-Energy Spectral CT

Dual Layer Detector Data Representation – Image Domain

$Z_{eff}\_1 > Zeff\_2 > Zeff\_3$

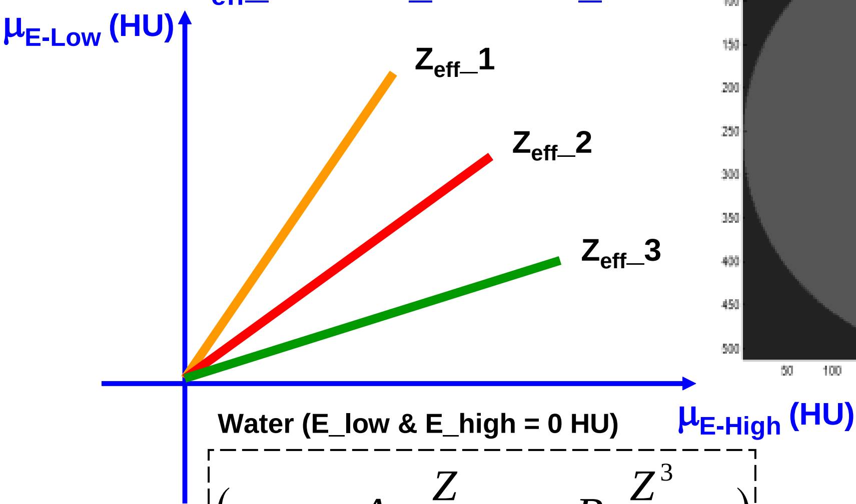

Water (E_low & E_high = 0 HU)

$$\left(\mu_{Z,E} \cong A \cdot \frac{Z}{E^{0.2}} \cdot \rho + B \cdot \frac{Z^3}{E^3} \cdot \rho\right)$$

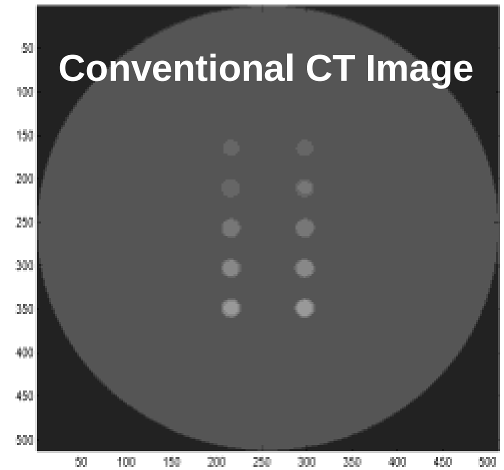

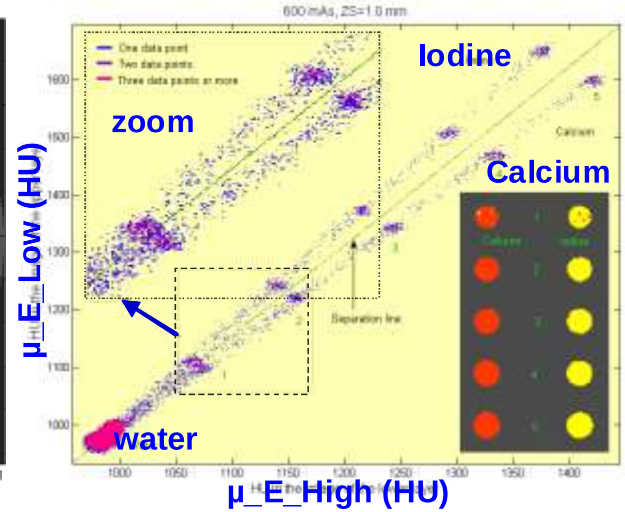

A phantom with different concentrations of Calcium and Iodine contrast agent

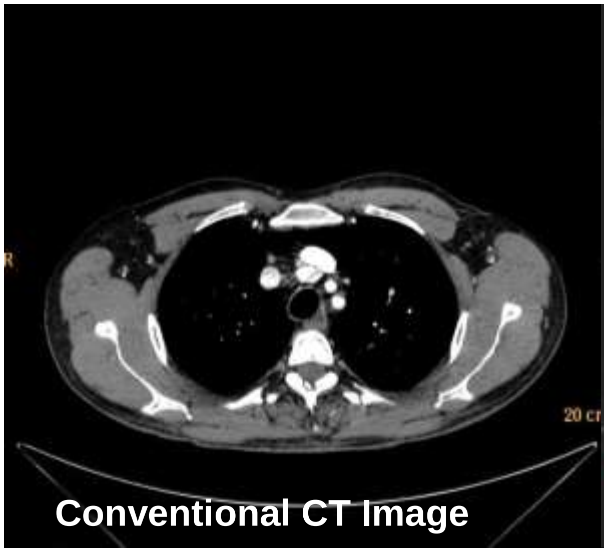

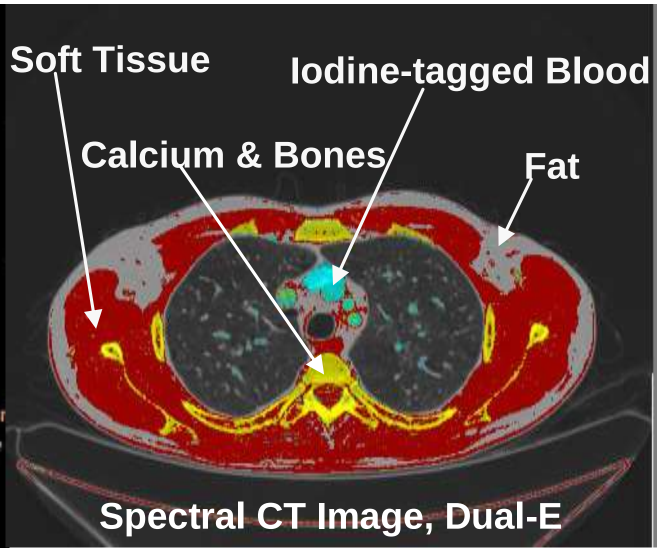

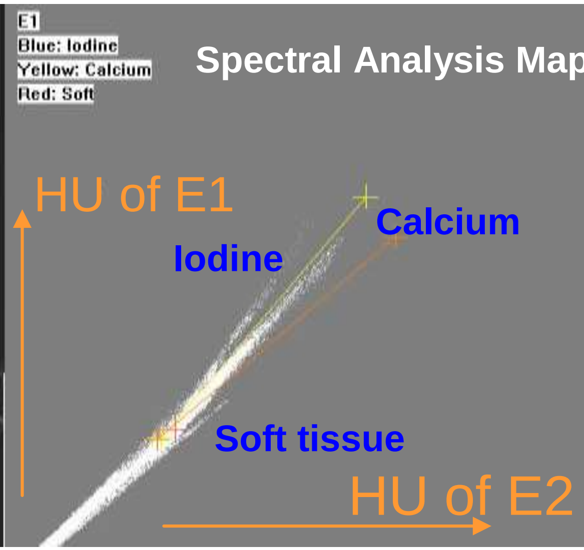

Dual-Energy Technologies – Various Vendors

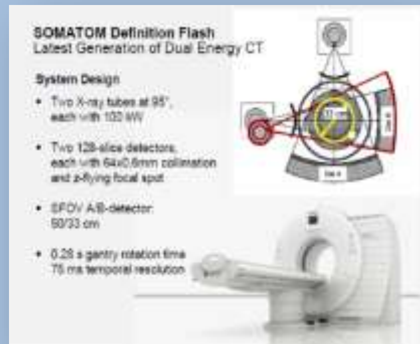

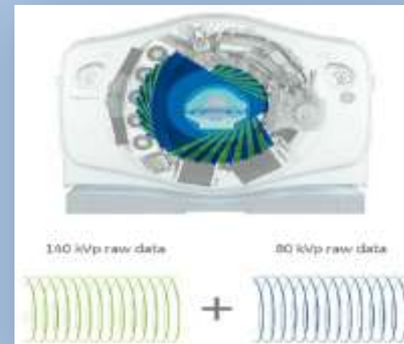

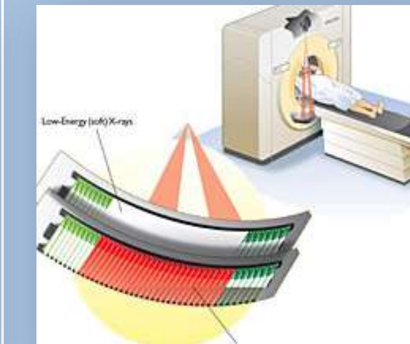

	Siemens	GE	Philips
Technology Path	Two-tube Two-Detector configuration	One tube with fast kV switching	One tube, detectors with simultaneous high and low energy discrimination
Full FOV	✗ Limited (~35 cm)	✓ Full (50 cm)	✓ Full (50 cm)
High/Low Energy Separation	✓ +	✓	✓✗
Projection Space Reconstruction	✗	✓	✓
Tube Current Modulation	✗	✗	✓
Low/High Energy Image Reconstruction	✓	✗	✓
Retrospective Dual-E Analysis, all protocols	✗	✗	✓

PHILIPS

Dual-Layer Spectral CT – Main Clinical Applications

Material Separation

- Direct CTA
- Gout Diagnosis
- Prep-Less CT Colonography

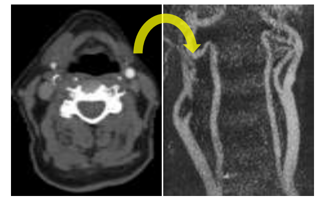

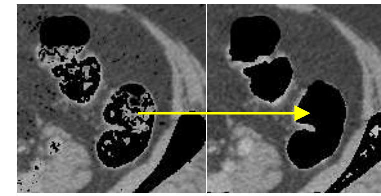

Material Quantification

- Virtual Non-Contrast
- Blood Flow Iodine Perfusion (PE)
- Lesion Uptake & Volume Assessment
- Plaque Characterization
- Cardiac CT
- Urinary Stone Characterization

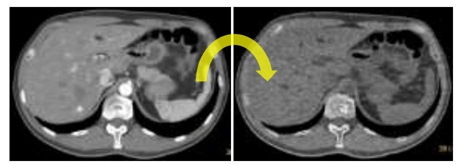

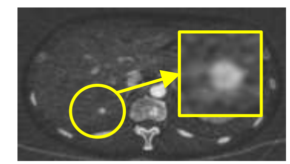
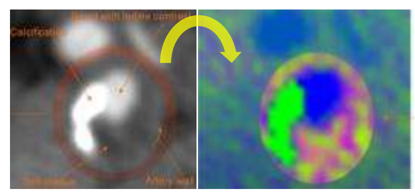
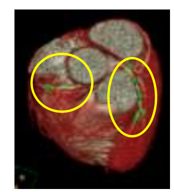
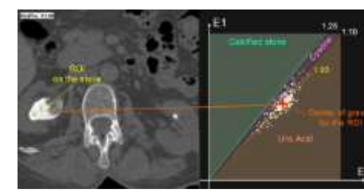

Monochromatic Imaging

- Salvaging Sub-Optimal CTAs
- Optimum CNR Imaging (↑Lesion visualization)
- Metal & Beam Hardening Reduction
- Effective Atomic Number

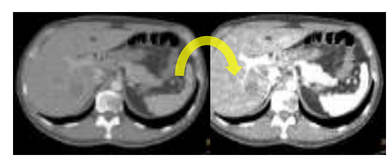
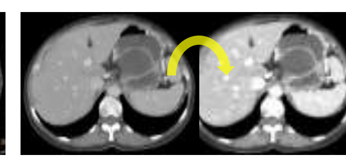
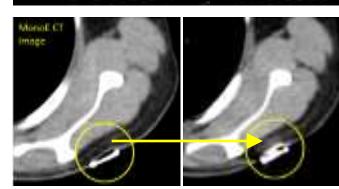
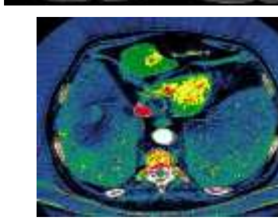

PHILIPS

Dual-Layer Spectral CT, Clinical Experience

Monochromatic Imaging

Lesion Characterizatio n

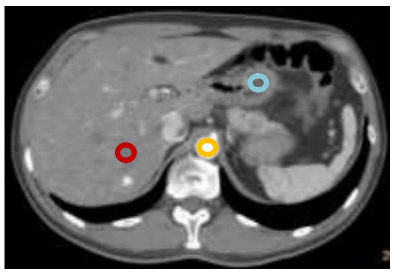

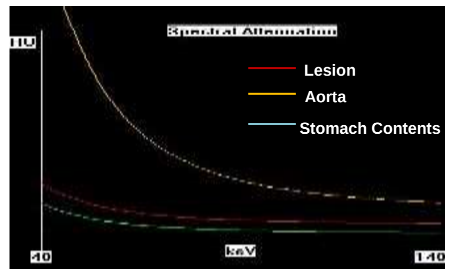

Material Decomposition

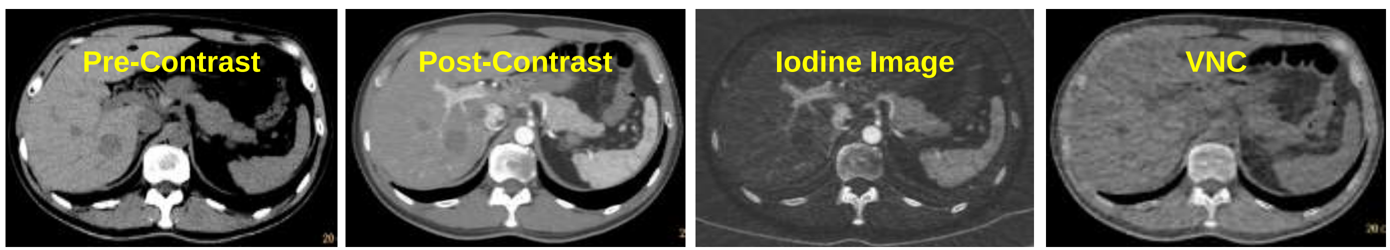

Material Decomposition (Color Display)

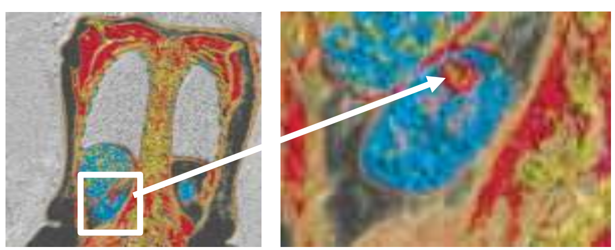

Dual-Layer Spectral CT, Viewer Screen Shot Example

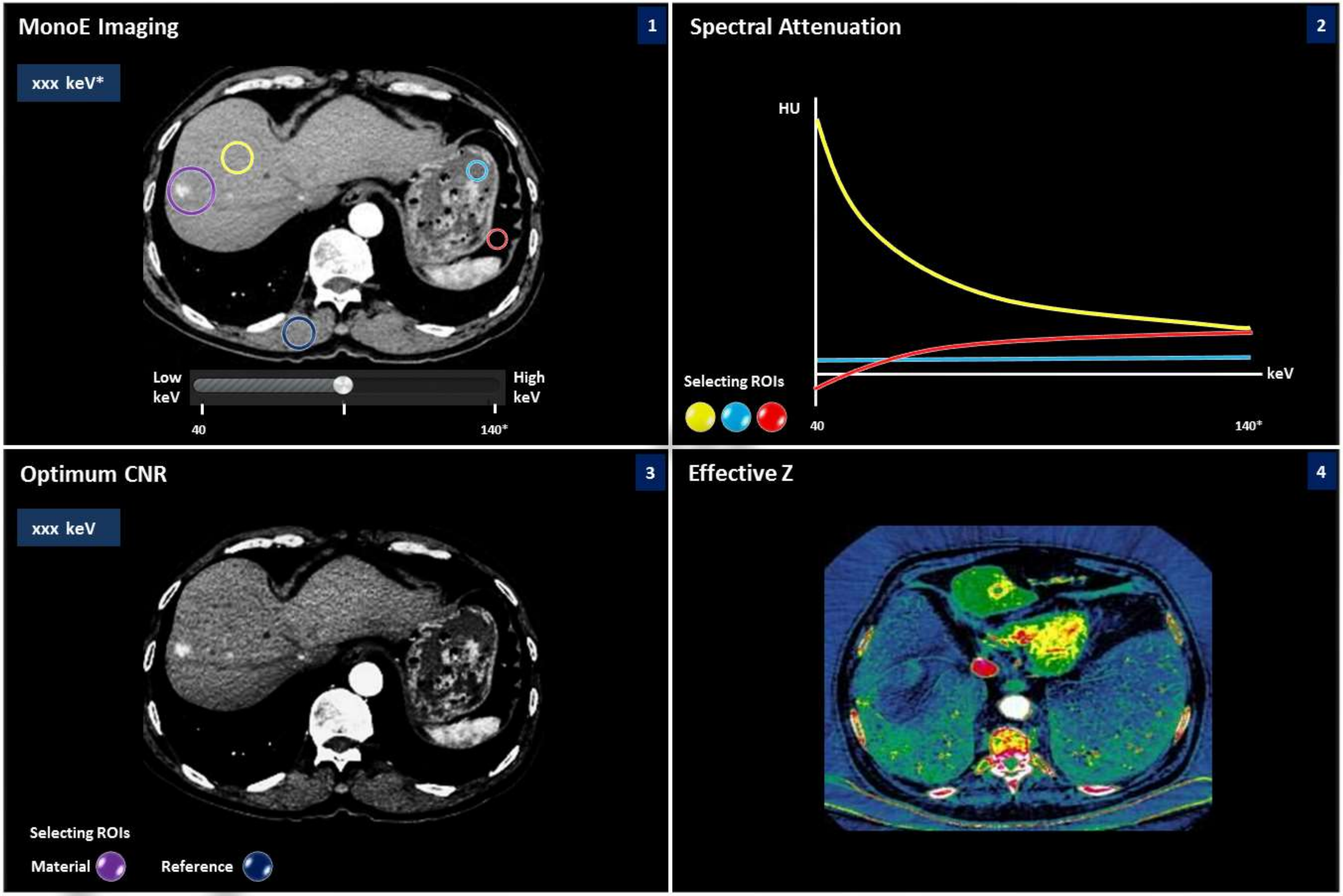

Photon-Counting Spectral CT – Photon-Counting Detector

Conventional Detector

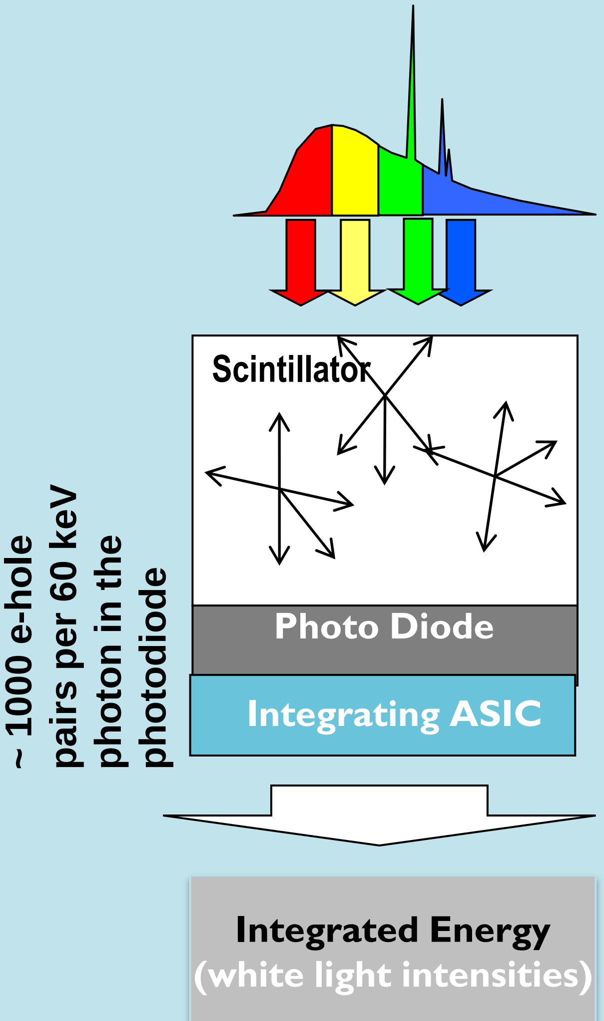

Direct Conversion Detector

High energy photons hit a semiconductor and are directly converted to an analog signal

A fast ASIC translates individual signal pulses to counts at several energy bins

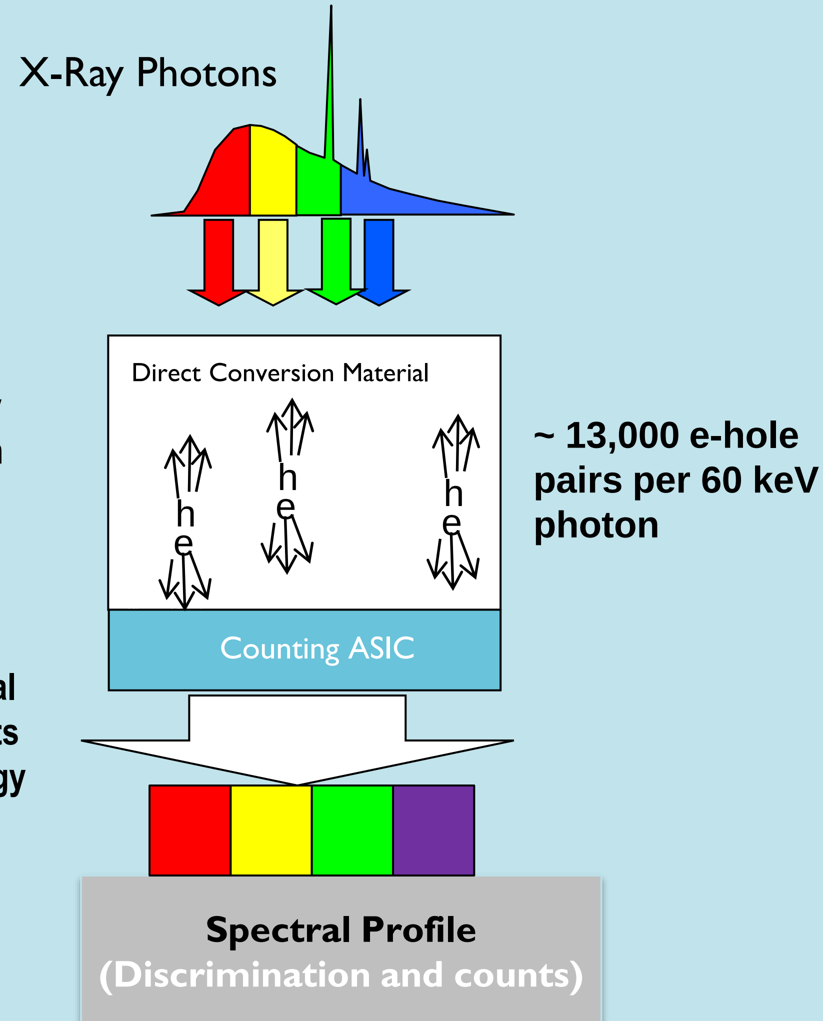

Photon Counting Detector Direct Conversion VS Energy Integration

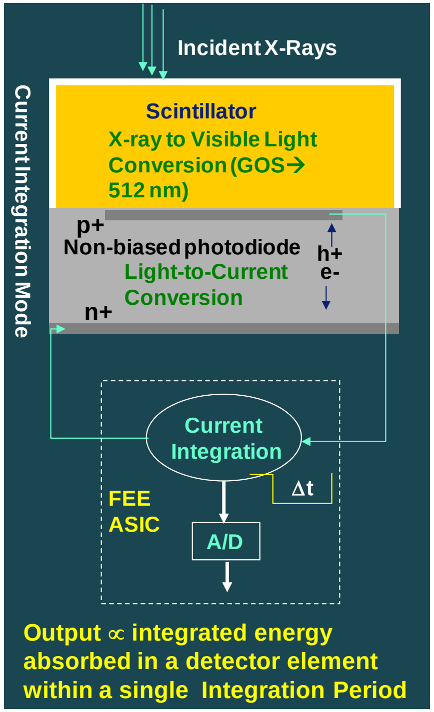

A Current-Integration CT Detector

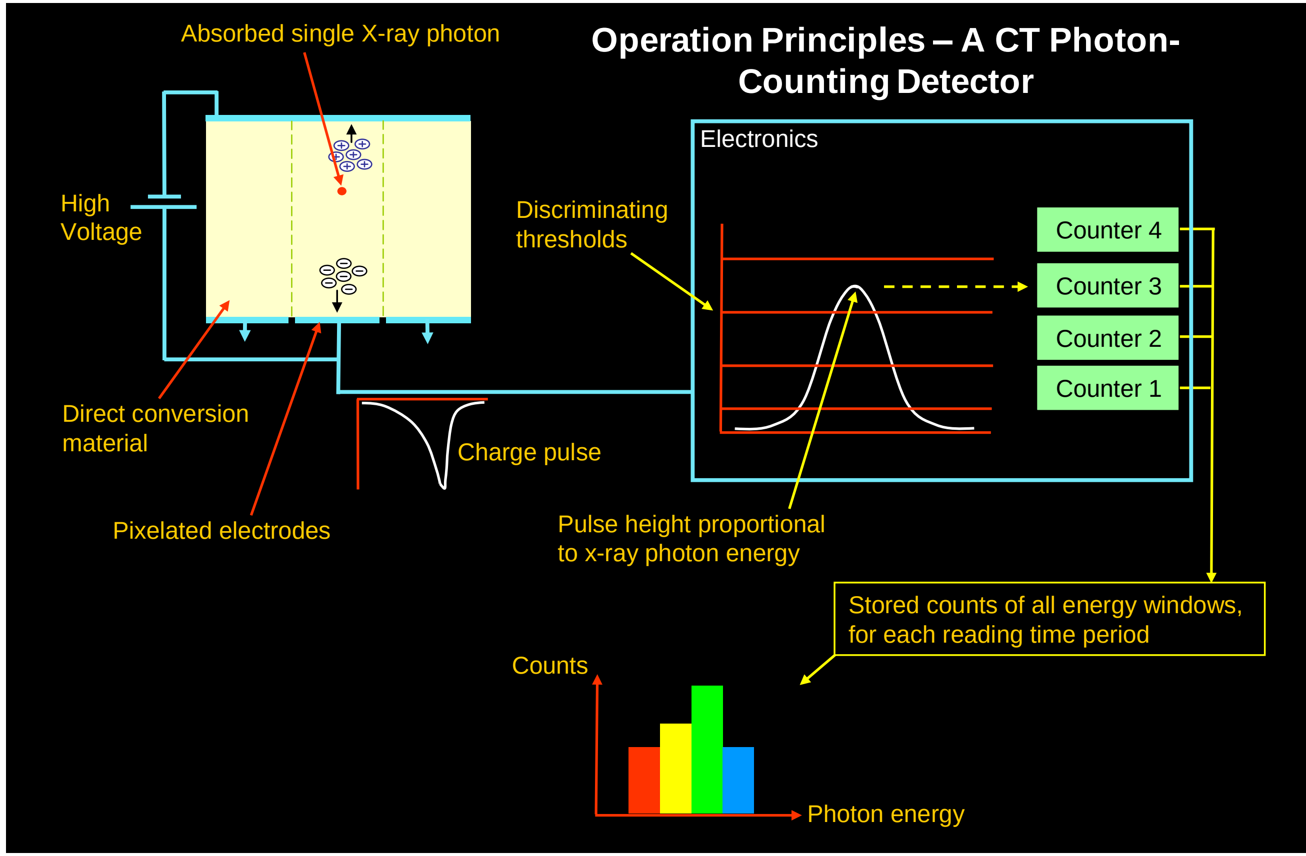

A Photon-Counting, Direct-Conversion, CT Detector

PhC Requires much smaller pixels to enable CT radiation rates

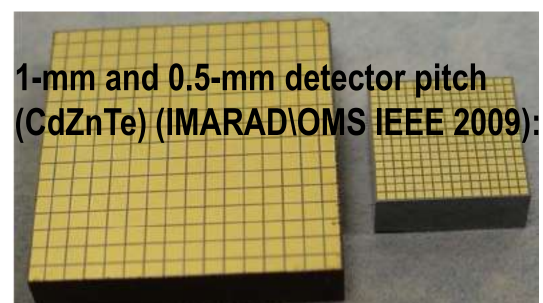

The Photon Counting Energy Weighting "Miracle"

$$S_{ph.c.} \propto \sum_{i=1}^{N_{bins}} 1 \cdot k_i \qquad S_{EI} \propto \sum_{i=1}^{N} E_i \cdot k_i \rightarrow \int_0^{\infty} E \cdot w(E)dE$$

$$\sigma_{ph.c.} \propto \sum_{i=1}^{N_{bins}} 1^2 \cdot k_i \qquad \sigma_{EI} \propto \sum_{i=1}^{N} E_i^2 \cdot k_i \rightarrow \int_0^{\infty} E^2 \cdot w(E)dE$$

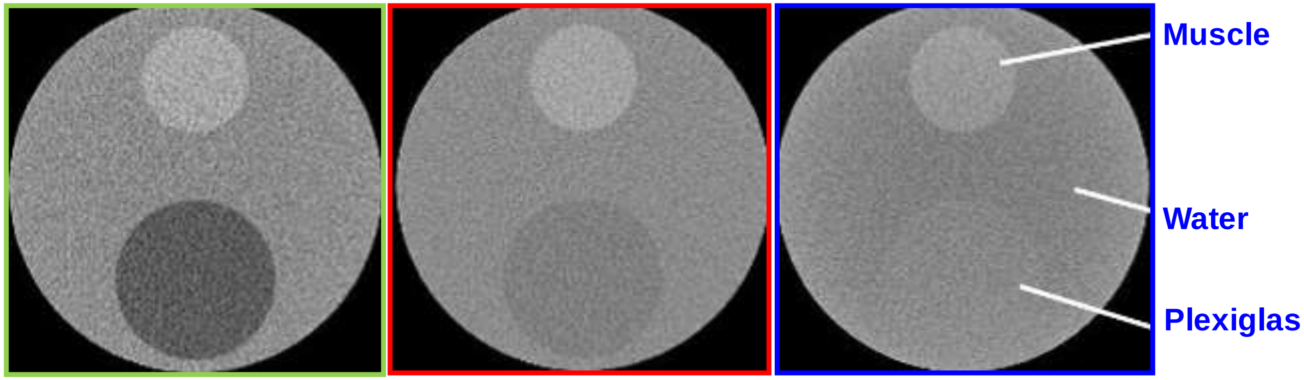

8 bins of 11-keV each: $1/E^3$ weighting

Photon-Counting total (no energy bins weighting)

Energy Integration

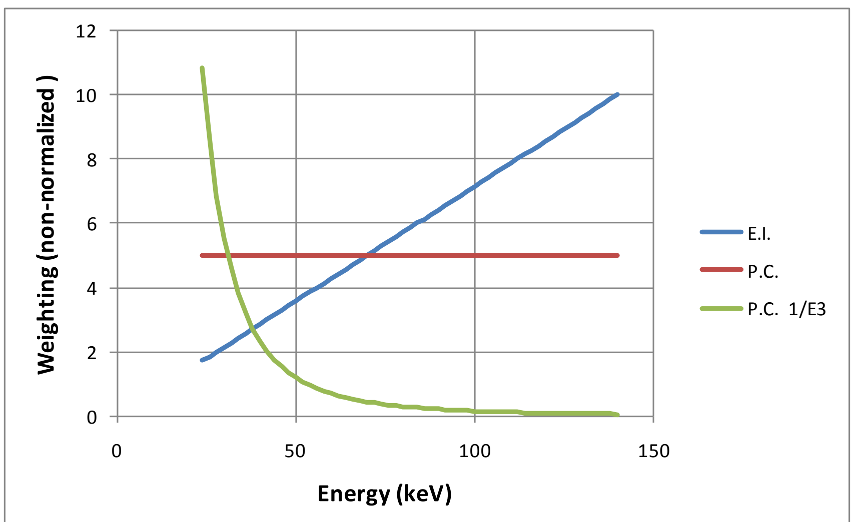

1. Z_eff of Plexiglas is ~20% < water
2. Energy Integrating over weights density over Z.
3. Photon Counting changes HU ratios, Contrast difference, and CNR
4. Opportunity to adapt energy weighting to specific applications
5. Potential increase in soft-tissue resolution.

Where Dual-Energy CT Fails – The Need for More than 2 Energy Bins.

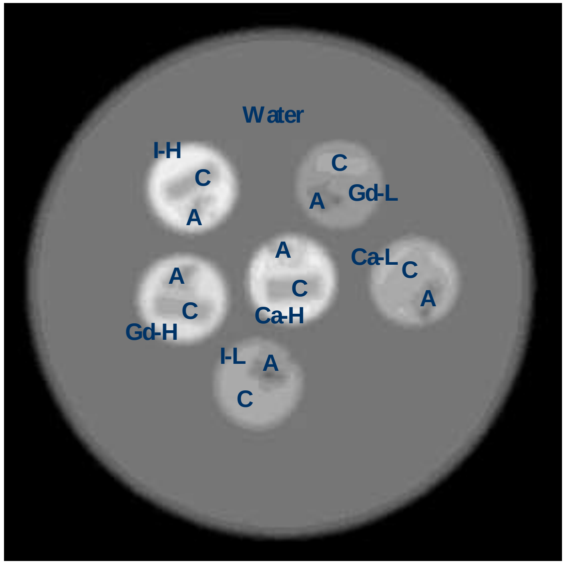

I – iodine
Gd – gadolinium
Ca – calcium (as CaCl)

H – high concentration
L – low concentration

C –solid carbon
A –air bubbles (in foam)

(Measured in a Rotating Table Photon Counting Mini CT, PHILIPS Healthcare, Haifa)

Mixtures or interfaces of more than 2 materials, suffers from spectral partial volume, distorting material decomposition and classification

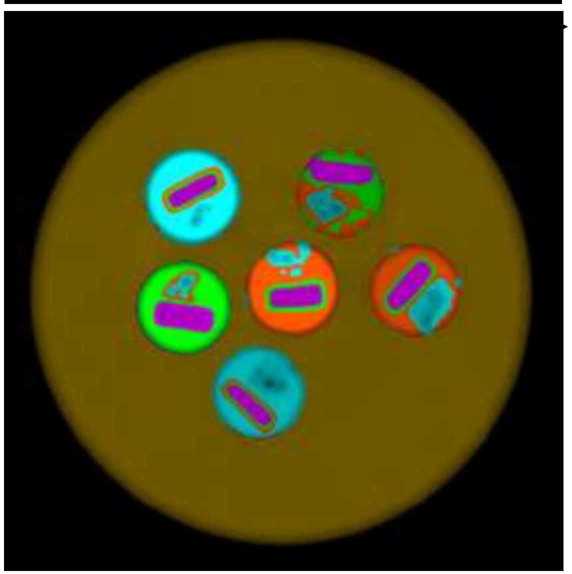

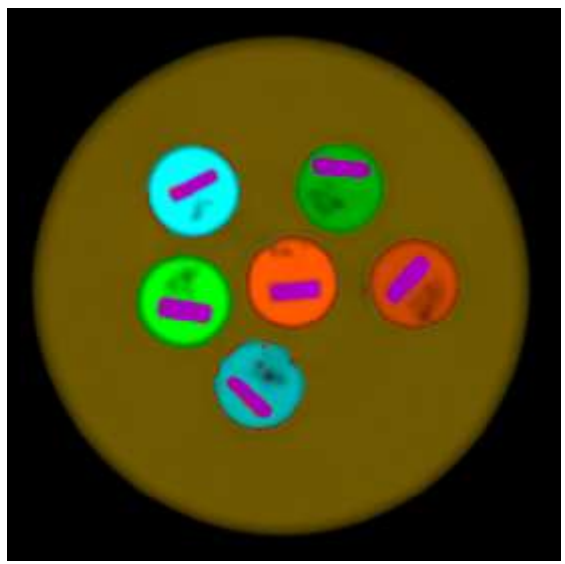

Iodine

Calcium Chloride

Gadolinium

Carbon

Water

<u>2 spectral windows:</u>
25-46, 85-125 keV

<u>6 spectral windows:</u>
25-46, 46-54, 54-65, 65-75, 75-85, 85-125 keV

PHILIPS

So Where is The Catch, Why CT is Not Transforming to Photon-Counting Detector?

1. **Best Candidates, CdTe and CdZnTe (CZT) are not easy to manufacture, to meet CT requirements**
2. **Detector Polarization (eliminating or distorting the electric field inside the detector, stopping any signal output), mainly caused by traps and impurities in the crystal lattice**
3. **Charge sharing between close neighboring pixels, causing low energy tail, that distorts measured energy spectrum, especially for a wideband spectrum like in CT**
4. **Te and Cd fluorescence K-escapes to neighbor pixels and from neighbor contributing to the low-energy tail**
5. **Pile-Up already at relatively low rate**

Pile-Up Issue in Photon Counting

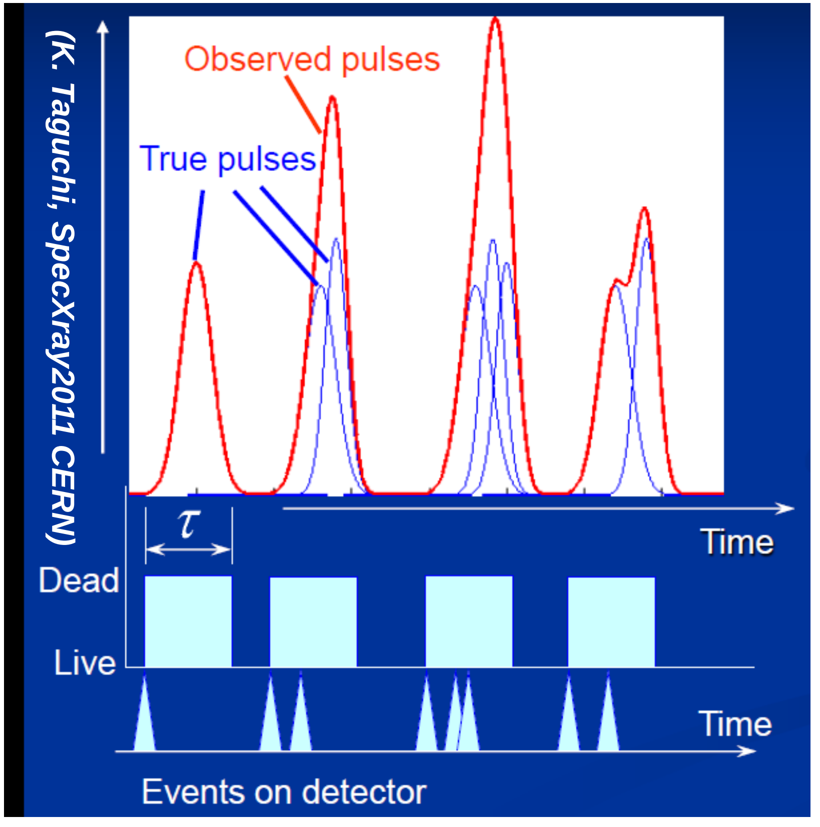

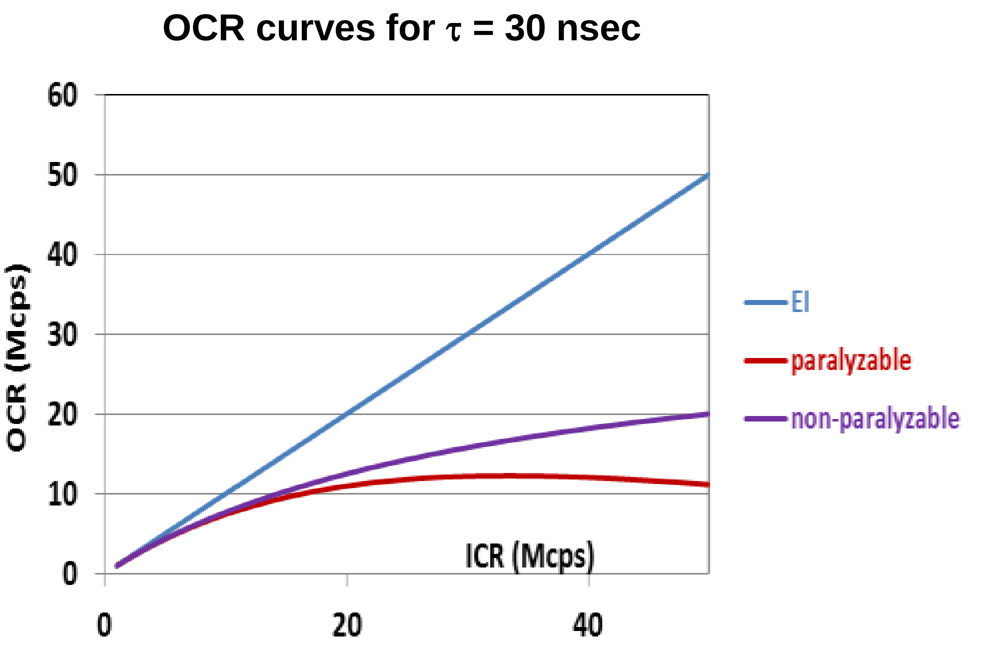

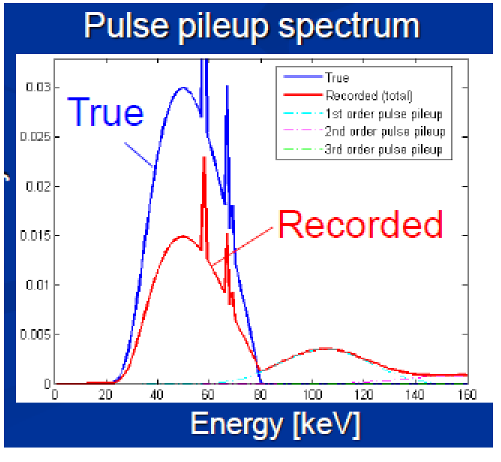

Paralyzable: $$\text{OCR} = ICR * \exp\left(-ICR * \tau\right)$$

Non-Paralyzable: $$\text{OCR} = \frac{ICR}{(1 + ICR * \tau)}$$

OCR=Output Count Rate
ICR=Input Count Rate

PHILIPS

DQE(0) in Photon Counting Detectors

$$\mathrm{DQE}(\nu) \equiv \frac{\mathrm{SNR}^2_{\mathrm{out}}(\nu)}{\mathrm{SNR}^2_{\mathrm{in}}(\nu)}. \Rightarrow \quad DQE = \left(\frac{\frac{\partial(OCR)}{\partial(ICR)} * \left(\frac{ICR}{\sqrt{(VAR)_{OCR}}} \right)}{\left(\frac{ICR}{\sqrt{VAR_{ICR}}} \right)} \right)^2$$

For Variance estimates see

Yu and Fessler in Phys. Med. Biol. 45 (2000) 2043-2056.

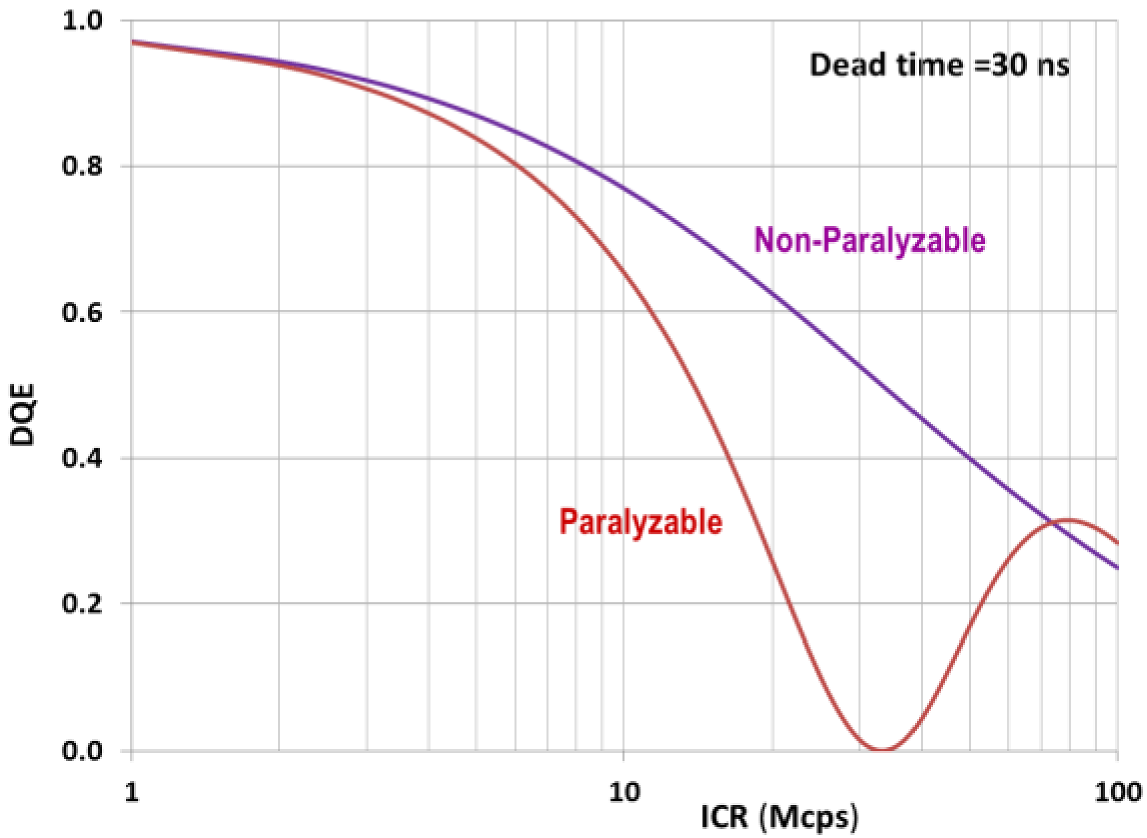

Low-Energy Tail and its effect on Spectral CT Quality

CdTe arrays: Spectral response to Am241 source (59.5 keV)

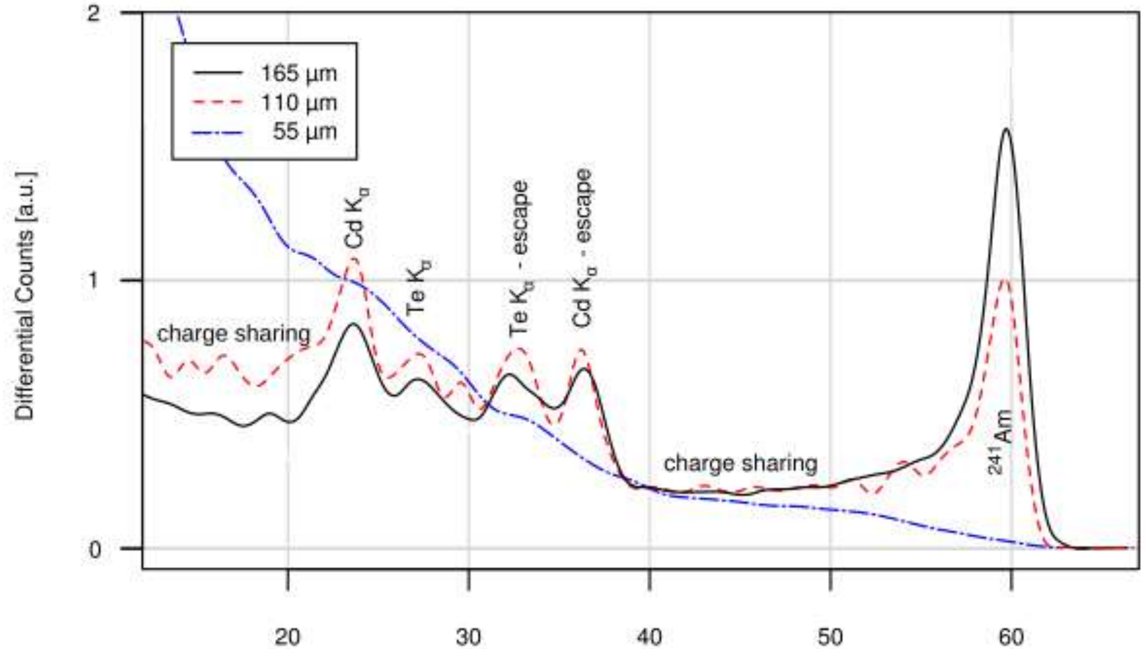

Figures taken from
T. Koenig et al
Phys. Med. Biol. 57 (2012) 6743–6759

CdTe arrays: Spectral Response to a 110 kVp X-Ray Tube

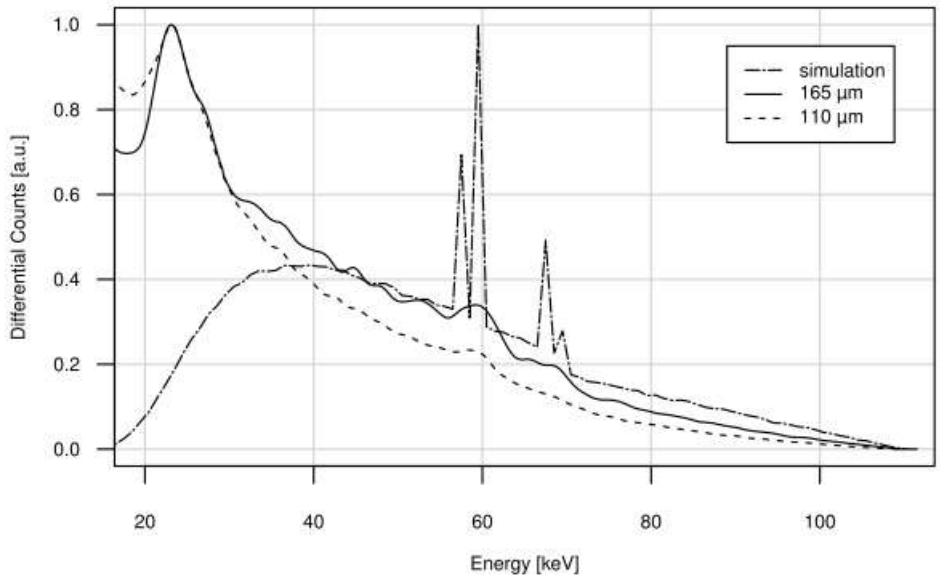

Pre-clinical spectral CT scanner platform

- Gantry with rotation speed up to 1/3 s per turn
- μ-Focus X-ray tube
  - 40 kVp - 130 kVp
  - max. 65W
- CdTe-based Photon-Counting detector
  - 0.4 mm pixel pitch, 1024 pixel along X
  - 6 energy bins per pixel
- Magnification: 2 - 6
- Field-of-view: 6 cm - 23 cm
- Spatial Resolution: 100 μm - 250 μm

First scanner: Philips Research Hamburg

Scanner copy: Washington University, St. Louis
G. Lanza, S. Wickline

PHILIPS

Enabling K-Edge Imaging and Targeted CT Imaging
(PHILIPS – Mount Sinai Collaboration)

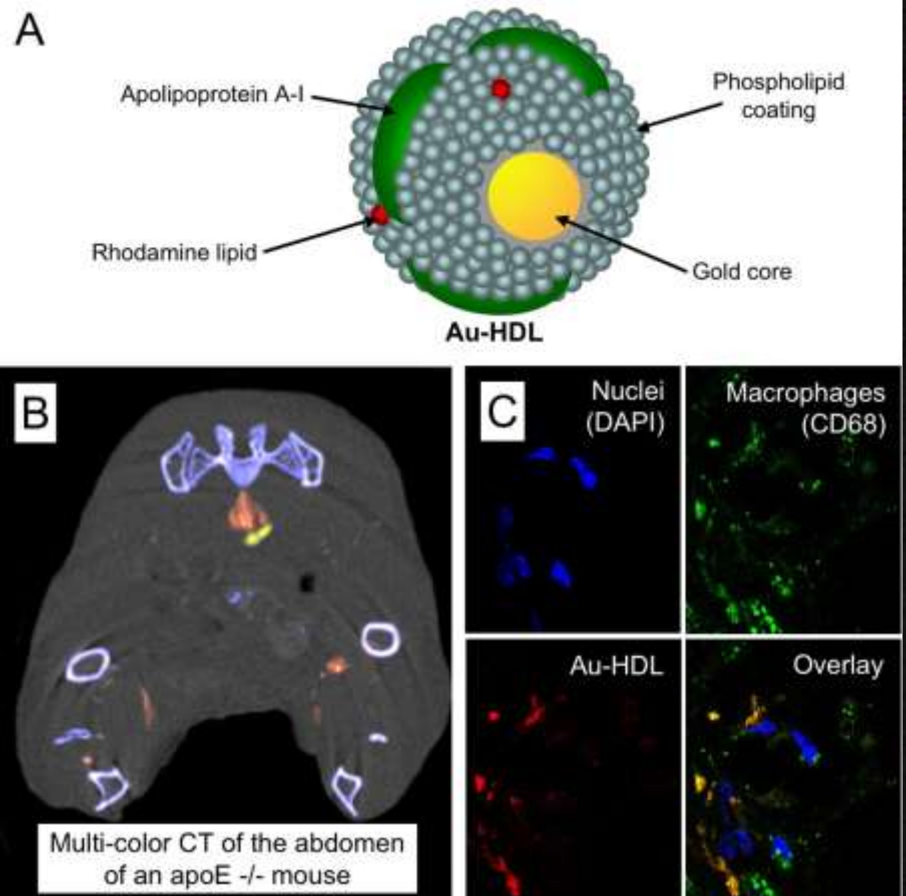

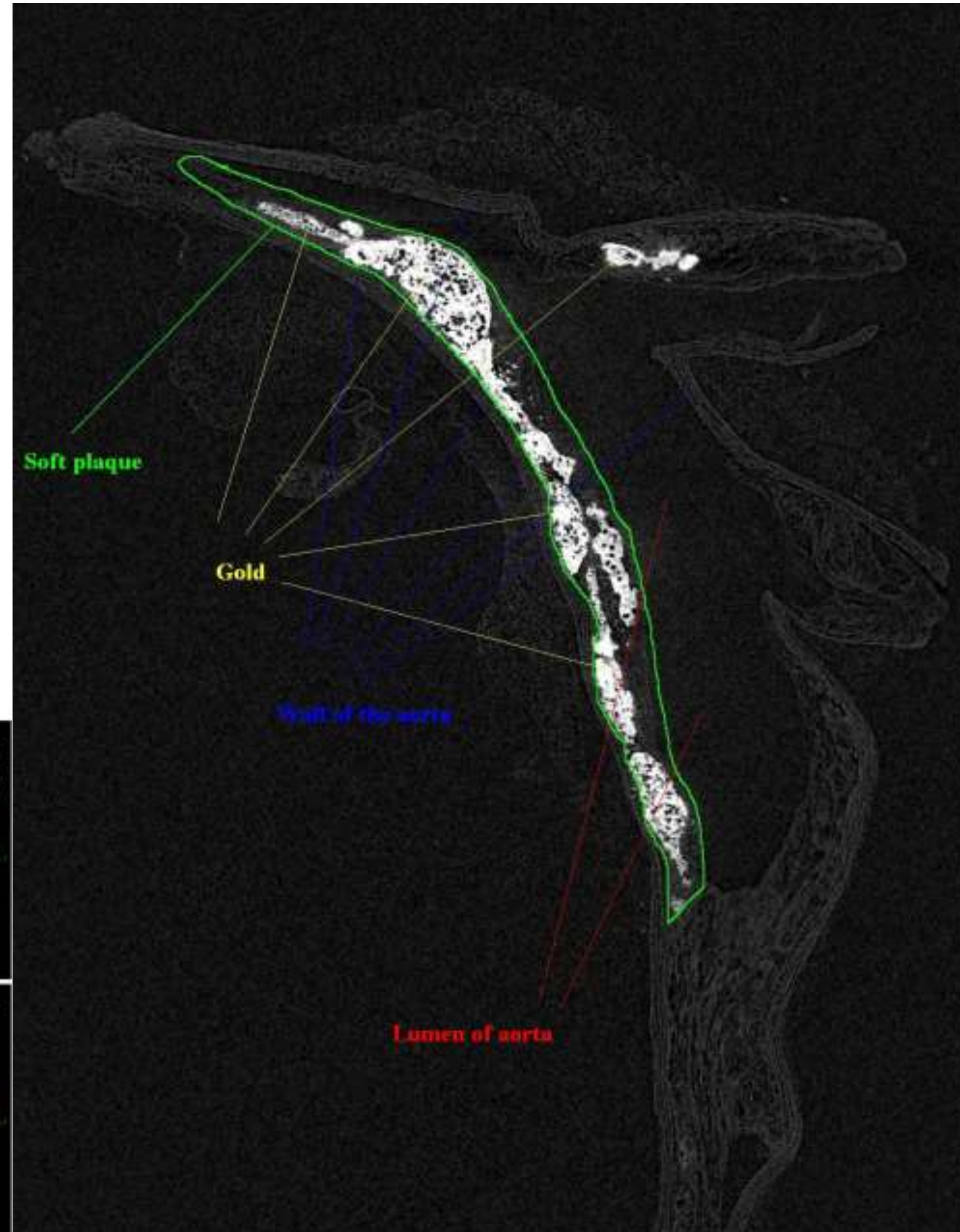

PHILIPS

Washington University Collaboration

Imaging nano particles, loaded with Gadolinium & Bismuth, and targeted mainly to fibrin in soft plaque

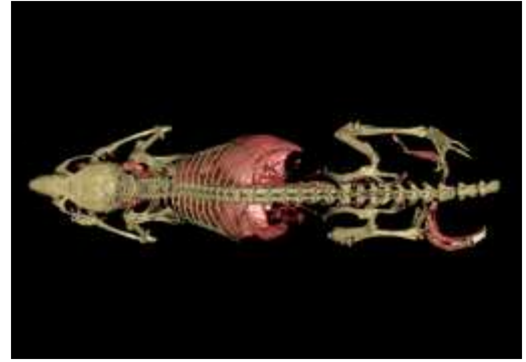

Anatomical mouse image with Iodine concentration overlay

Human carotid samples with targeted contrast agent

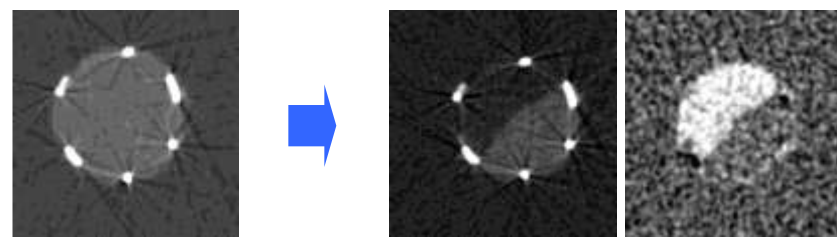

Artificial calcification inside of a stent.
Left: integrated CT image, Right: photo- and Gd image

Hepatis steatosis (fatty liver)
phantom measurements

30

imaging results

From collaboration with Eindhoven

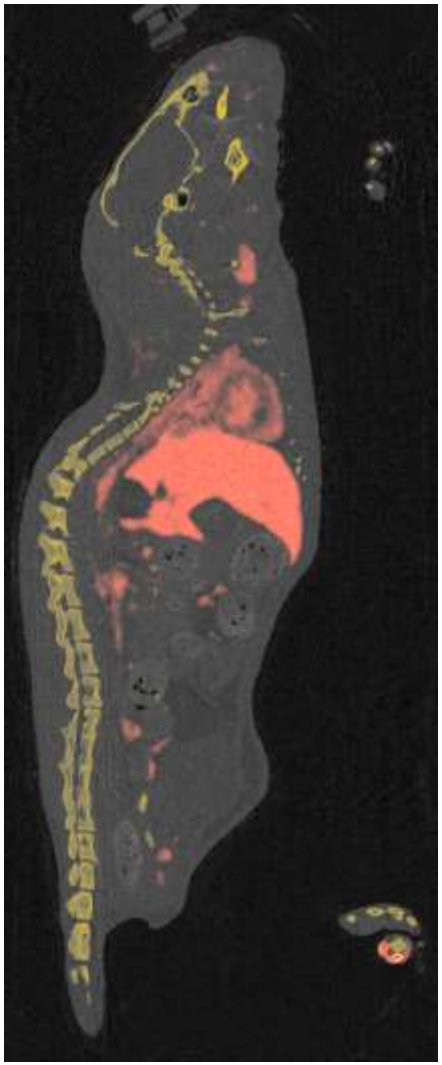

- iodinde-based bloodpool agent
- mouse images

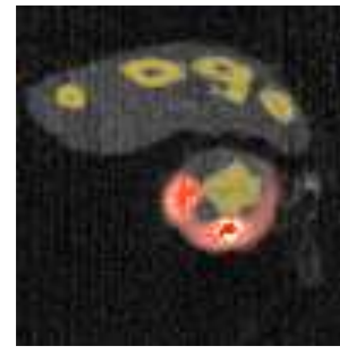

Tail cross section

organ	view	ρ_I [μg/mm^3]
liver	c	4.6 ± 0.2
spleen	c	4.0 ± 0.3
kidney	c	1.9 ± 0.2
heart	s	2.9 ± 0.2
liver	s	4.5 ± 0.2

Quantification

31

Investigating K-Edge Imaging at WashU

Bismuth Nanobeacons Target Fibrin of Thrombus on Ruptured Plaque

Applications demand high delivered payloads of heavy metals targeted to intraluminal thombus, but excluded from intraplaque fibrin.

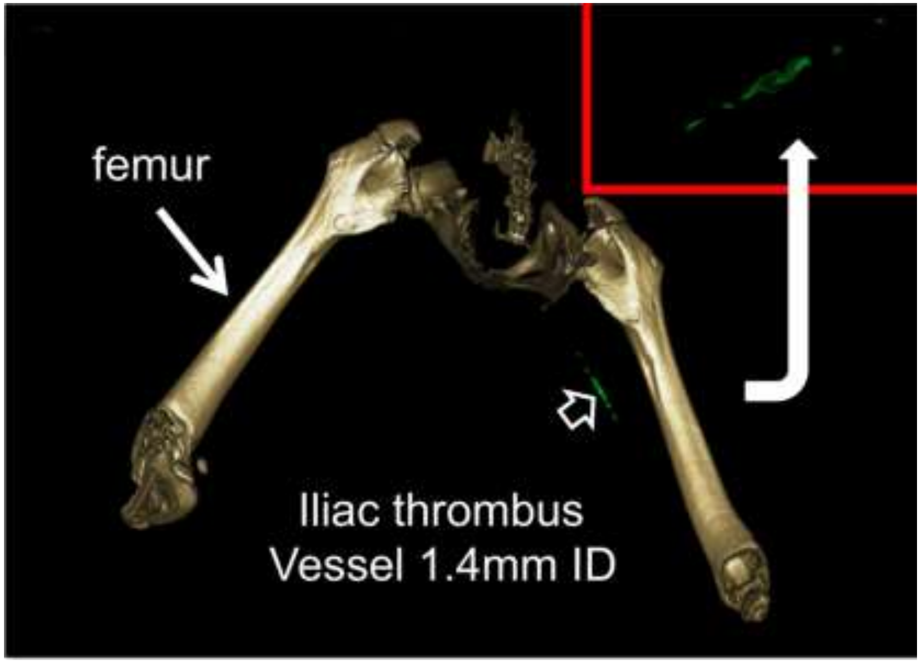

NanoK targeted to thrombus in situ. Systemic targeting studies on-going in vivo

fluorescence microscopy optical microscopy

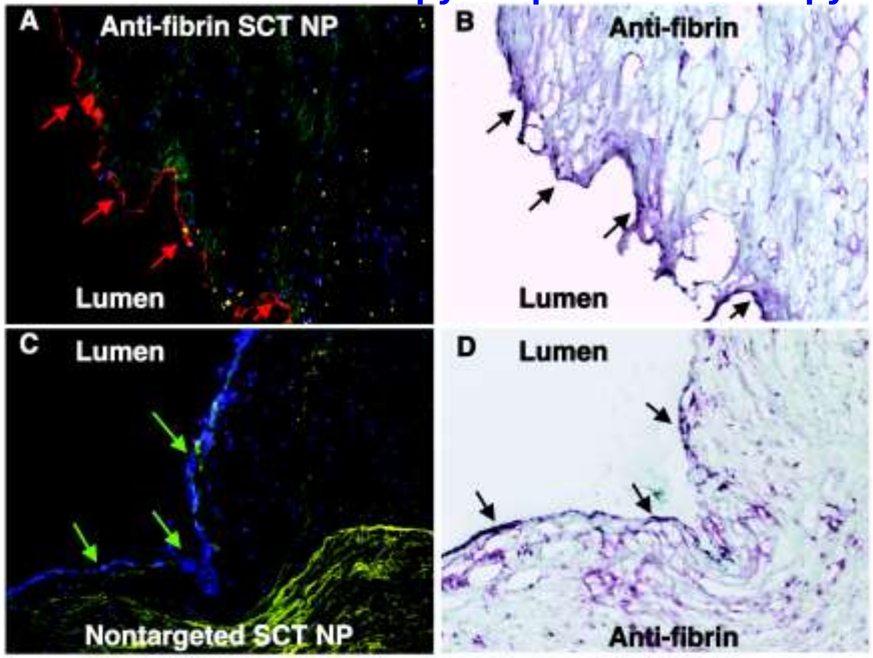

Nanoparticles home specifically to intra-lumenal fibrin not intramural fibrin from healed hemorrhage or rupture
(in vitro CEA specimens from Patient)

Pan, Roessl, Thran,…Proksa, et. al. *Angew Chem Int Ed.* 2010, 9635-39

PHILIPS

Investigating K-Edge Imaging at WashU

Imaging of new Ytterbium Nanobeacons

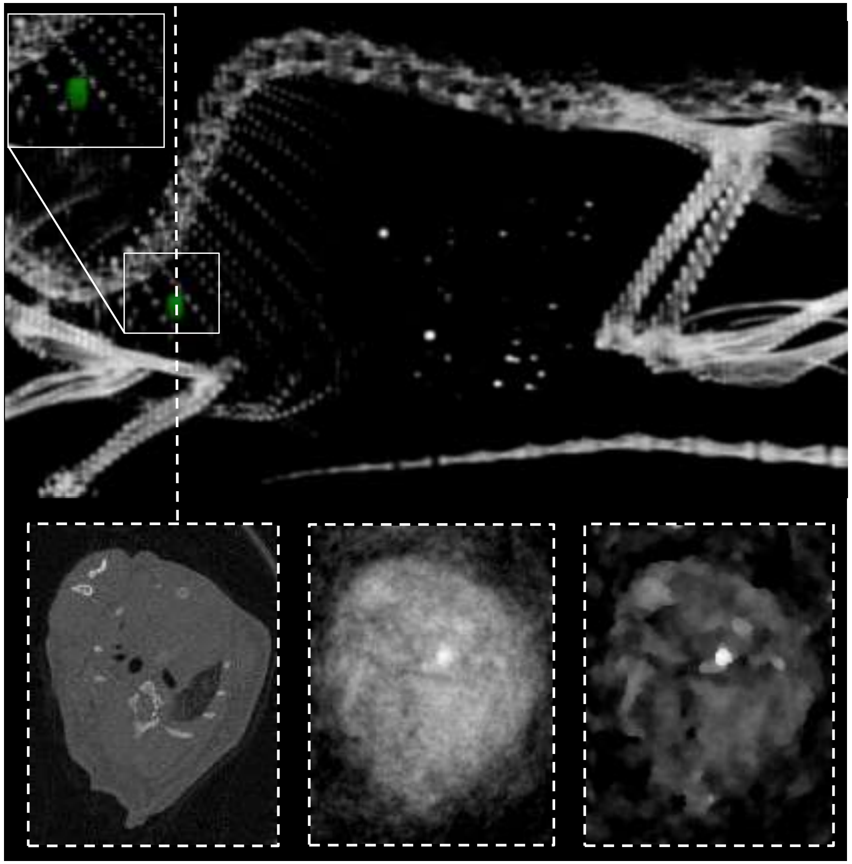

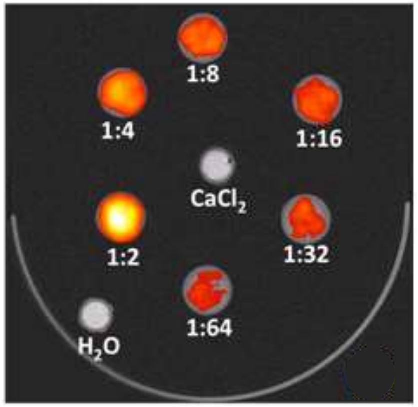

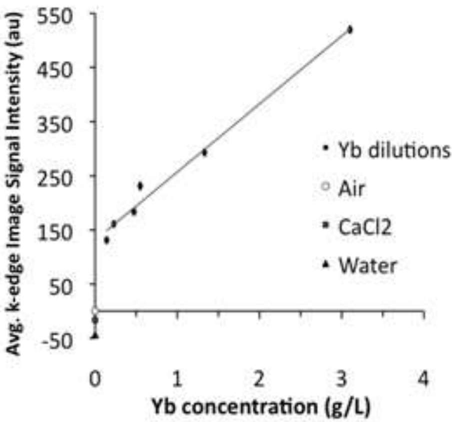

Pan, Schirra, Roessl, Thran, … ,Proksa et al., ACS Nano. 2012 (in press, e-pub available)

Consequences

1. **Innovative detectors technologies has lead, and will lead future CT evolution and revolution towards quantitative imaging in more than just anatomy and morphology.**

2. **Detector-based spectral CT enables the benefit of material\tissue analysis retrospectively for all conventional protocols, without the need to decide on a specific Dual-Energy protocol.**

3. **Photon-Counting detectors for spectral CT imaging is a promising technology, that offers also much better spatial resolution, no electronic noise, better CNR, capability to further reduce dose, and a more accurate material and tissue representation and decomposition.**

4. **Photon-counting CT may open an opportunity to use targeted contrast agent, thus become more quantitative, enabling more personalized diagnostics.**

5. **We are not yet there. There are several significant technology challenges, in detector performance and pile up issues, to overcome.**

PHILIPS